N.A.E.

NATIONAL AERONAUTICAL ESTABLISHMENT
LIBRARY

R. & M. No. 2685
(11,944, 12,650, 12,147)
A.R.C. Technical Report

MINISTRY OF SUPPLY

AERONAUTICAL RESEARCH COUNCIL
REPORTS AND MEMORANDA

A Comparison of Two Methods of Calculating Wing Loading with Allowance for Compressibility

By

V. M. Falkner, B.Sc., A.M.I.Mech.E.

with Appendix:

Note on Falkner's Method for Calculating Compressibility Effects on Wing Loading

By

W. P. Jones, M.A., of the Aerodynamics Division, N.P L

Crown Copyright Reserved

LONDON: HER MAJESTY'S STATIONERY OFFICE
1953
FIFTEEN SHILLINGS NET

A Comparison of Two Methods of Calculating Wing Loading with Allowance for Compressibility

By
V. M. Falkner, B.Sc., A.M.I.Mech.E.*

with Appendix:

Note on Falkner's Method for Calculating Compressibility Effects on Wing Loading

By
W. P. Jones, M.A.,†
of the Aerodynamics Division, N.P.L.

Royal Aircraft Establishment
21 SEP 1953
LIBRARY

Reports and Memoranda No. 2685
October, 1949

Summary.—The report gives the results of a comparison by two different methods of the aerodynamic loading of a tapered V wing of aspect ratio 5·8 and 45 deg sweepback at $M = 0 \cdot 8$, based on the Prandtl-Glauert factor or linear perturbation theory; the first method, associated particularly with vortex-lattice theory, deals with changes in Mach number by preserving the plan of the wing and using special Tables of downwash, while the second uses the solution for Mach number 0 on a wing with the lateral dimensions reduced by a specified factor.

The two methods are shown to be in good general agreement at $M = 0 \cdot 8$ and, although it can be argued that the second method is more accurate on theoretical grounds, this is offset by the fact that the first has considerable advantages in ease of calculation, and in the possibility of extension to more accurate solutions when the Prandtl-Glauert factor fails at high subsonic speeds.

Examples of the application of the theory are also given for a delta wing, for a straight tapered wing without sweep, and for a tapered wing with 28·4 deg sweepback. It is possible to give a general and reasonable explanation of the nature of the variations of load grading and local aerodynamic centre which occur with increasing Mach number, and with the information given, there should be no difficulty in the prediction of Mach number effects on a wide range of plan forms.

Since the completion of the work, a mathematical examination of the limitations of the first method has been made by W. P. Jones who has calculated exact values of downwash due to a rectangular vortex over a range of Mach numbers for comparison with those obtained by the approximate formula. His work, which is included as an Appendix, confirms the accuracy of the approximate method at high Mach numbers.

---

1. *Introduction.*—The object of this work is to compare two methods of calculating wing loading with allowance for compressibility and to give examples of their use. The first method, based on the use of special tables of downwash, is described in Ref. 1, where the results of calculations carried out on a swept-back tapered wing by the use of standard solutions omitting the effect of the centre-line correction are also given. The second method depends on the direct use of the Prandtl-Glauert factor, which involves a reduction in the lateral dimensions of the wing.

* {A.R.C. 11,944. 25th November, 1948.
{A.R.C. 12,650. 15th October, 1949.
† A.R.C. 12,147. 7th February, 1949.

(22975) A

2. *Theory: First Method.*—The first method is based on the following argument. The effect of the Prandtl-Glauert factor[2] is that each unit of bound vorticity which represents the lifting plane in two-dimensional flow is increased for a given incidence in the ratio $1/\sqrt{(1 - M^2)}$. It follows that the potential theory on which the vortex-lattice method is based is no longer valid, because there is the equivalent of added vorticity without a corresponding addition to the downwash. The adaptation to vortex-lattice theory is made in the following way. As far as the bound vorticity along any chord at Mach number M is concerned, the calculated downwash at the wing surface will be correct if it is assumed that $\sqrt{(1 - M^2)}$ of the total vorticity acts in accordance with potential theory, while the remainder $1 - \sqrt{(1 - M^2)}$ is without potential field. The same considerations do not apply to the trailing vorticity as it has been shown by A. D. Young[3] that, in lifting-line theory, the downwash field at the wing due to the trailing vorticity is not affected by compressibility. Young's result is only strictly applicable to lifting-line theory, but if the approximation be made that this result can also be used in lifting-plane theory, a simple solution of the problem is possible. It is only necessary to work out two sets of equations for the wing, one set being the standard equations derived from the complete tables of downwash and corresponding to $M = 0$, and the other set being derived by the use of tables of induced downwash and corresponding to the hypothetical case $M = 1$. The equations corresponding to any Mach number M are then obtained by summing the proportions $\sqrt{(1 - M^2)}$ of set (1) and $1 - \sqrt{(1 - M^2)}$ of set (2).

2.1. The factors of induced downwash are obtained in the same way as the factors of complete downwash, but with the omission of the downwash contribution due to the bound vortex. These factors have been calculated by a formula which is readily deduced from Fig. 3 of R. & M. 2591[4] and are given in Tables 30 to 40.

2.2. *Second Method.*—The second method is based on the Prandtl-Glauert rule or linear perturbation theory by which, if the velocity variations are small, the effects of Mach number can be represented by an equivalent solution for $M = 0$ for a wing for which the lateral and vertical dimensions have been reduced by appropriate factors. The formulae for this method have been collected together and presented in a concise and clear form by R. Dickson in Ref. 5. For the work now under investigation, which includes incidence and wing twist solutions, the process reduces to a simple alteration of the lateral dimensions of the wing in the ratio $\sqrt{(1 - M^2)}$, the solution of this distorted wing for $M = 0$, and the application of the following transformation:—

(a) The circulation $K/4sV$ per radian or load coefficient $C_K = C_{LL}c/C_L\bar{c}$ plotted against η is correct.

(b) C_{LL}/C_L plotted against η is correct.

(c) The position of the aerodynamic centre is correct.

(d) The value of $dC_L/d\alpha$ is to be multiplied by $1/\sqrt{(1 - M^2)}$.

(e) The incidence for zero lift, α_0, is correct.

(f) The moment coefficient at zero lift, C_{m0}, is to be multiplied by $1/\sqrt{(1 - M^2)}$.

3. *Results—45 deg Tapered Wing.*—The calculations, apart from the use of the special tables of downwash, have been carried out precisely in accordance with the standard method described in R. & M. 2591[4] and 2596[6], and consist of three, six, or nine-point solutions with or without auxiliary solutions to allow for the centre-line correction.

The main effort has been directed to solutions for a tapered wing, with taper ratio of 0·25 to 1, aspect ratio 5·8, and 45 deg sweepback, as shown in Fig. 2, the choice being influenced by the fact that the wing is the subject of an investigation including pressure plotting at the Royal Aircraft Establishment. After reduction of the lateral dimensions by a factor corresponding to $M = 0{\cdot}8$, the wing becomes of aspect ratio 3·5 with 59 deg sweepback.

Some of the work on this wing was done by the 84-vortex lattice before the standardisation of the 126-lattice and, although the former work is now obsolete, it still has value in its relation to the general accuracy of the method, and so has been placed on record.

The following solutions, which are given in Tables 7 to 27, have been calculated for the pair of wings:—59 deg wing, $M = 0$, 84-vortex, 3, 6, 9 and 12-point standard solutions; 126-vortex, 3, 6 and 9-point standard solutions and 6-point solution with centre-line correction; 126-vortex, 6-point standard solution with and without centre-line correction for wing twist, θ linear: 45 deg wing, $M = 0$, 126-vortex 9-point standard solution, and 6-point standard solution with and without the centre-line correction; 126-vortex 6-point standard solution for wing twist, θ linear, with and without centre-line correction; 45 deg wing, $M = 0{\cdot}8$, 126-vortex, 9-point standard solution and 6-point standard solution with and without centre-line correction; 126-vortex 6-point standard solution for wing twist, θ linear, with and without centre-line correction; 45 deg wing, $M = 1$, 126-vortex 6-point standard solution for wing twist, θ linear. Generally, the least accurate are the simpler 3-point solutions, and the most accurate given here are the six-point solutions with centre-line correction.

3.1. Selections from these solutions have been plotted in Figs. 3 to 9 with the object of demonstrating features of particular interest. For example, the first one, Fig. 3, deals with the convergence of the load coefficient C_K and local aerodynamic centre for the 59 deg wing. Considering first the load coefficient, it will be noted that all solutions, excepting the 84/9 and 84/12, are in good agreement, and the reason for the failure of the two latter is that they make use of control points over the front part of the wing at which the downwash values calculated for a given mesh of lattice are known to be less accurate than those over the rear part of the wing. This matter has been referred to in a previous report, and it is very satisfactory to note that, when this source of error is removed the remaining solutions, in spite of the differences in numbers of control points and the variations in the lattice, show remarkable agreement and leave no doubt that the standard solutions—although not the final solutions—have converged to a limit. As regards the local aerodynamic centre, the 3-point solutions are, of course, out of the question, and, if the 84/9 and 84/12 are omitted it is found that the 126/6 and 126/9 are in near agreement, but that the 84/6 does not quite reach the other curve. It is a fair deduction which does not at this stage require further proof that the 126 standard solutions for aerodynamic centre have converged to limits which are close enough for the present application.

As the centre-line correction will for reasons of economy be based on 6-point solutions, Figure 4 is devoted to evidence that there is little difference between 6 and 9-point solutions. The comparison is made for the 59 deg wing at $M = 0$, and for the 45 deg wing at $M = 0$ and $0{\cdot}8$, and, in each case, although there is a slight variation in the aerodynamic centre near the tips the solutions have converged for all practical purposes.

Figs. 5, 6 and 7 show the effect of the auxiliary solution or centre-line correction in the three cases, both incidence and wing twist solutions being included. The effects are similar in all cases, the local aerodynamic centre showing a movement aft in the central region and the load coefficient for the incidence solutions showing a drop at the centre with accompanying variation along the span, and for the wing twist solutions hardly any change. The effects of these changes on overall aerodynamic centre can be studied from the results given in R. & M. 2596[6].

3.2. The final comparison of the two methods has been carried out by using the six solutions, three for incidence, and three for wing twist, numbers 27, 29, 32, 34, 37 and 39, which are based on the 126-vortex pattern with centre-line correction. The comparison between the two methods depends on the agreement between the curves for C_K and local aerodynamic centre as given by solutions 27 and 37 for incidence and 29 and 39 for wing twist at $M = 0{\cdot}8$, but, to complete the work, and to show the variation which occurs between $M = 0$ and $M = 0{\cdot}8$, solutions 32 and 34 have also been included. The solutions for incidence are plotted in Fig. 8, and for wing twist in Fig. 9 and excellent agreement is shown throughout excepting that there is a slight variation in the locus of the aerodynamic centre for the incidence solution near the tip. This variation is a measure of the inaccuracy caused by the assumptions on which the first method is based. It would be quite easy to make allowance for this difference, but the effect should not be over-rated, because, occurring as it does in the region of rapidly decreasing circulation, the overall effects are small. This is shown in Table 28, where are collected together the main results for the six solutions, and from which it is concluded that the overall agreement between the two solutions is highly satisfactory.

4. *Results—Straight Tapered Wing.*—For the straight tapered wing, Fig. 1, the following solutions have been calculated:—$M = 0$, 6 and 9-point standard solutions for incidence, and 9-point standard solution for wing twist, $c\theta$ linear; $M = 0 \cdot 8, 0 \cdot 9, 1 \cdot 0$, 9-point standard solution for incidence; $M = 0 \cdot 9$, 9-point standard solution for wing twist, $c\theta$ linear. The results are given in Tables 1 and 2, and plottings of load coefficients and local aerodynamic centre for incidence solutions have been made in Fig. 10. It will be noted that, as far as the load coefficient and local aerodynamic centre are concerned, there is no appreciable difference between the 6 and 9-point solutions, numbers 1 and 2. The main conclusions to be drawn from Fig. 10 are the small change in the load coefficient between $M = 0$ and $0 \cdot 9$ and the regular forward movement of the local aerodynamic centre. Between $M = 0 \cdot 9$ and $M = 1 \cdot 0$ there is a more rapid change which is not genuine, being due to a breakdown of the method. Supporting evidence of this breakdown is that compressibility effects are approximately equivalent in a straight wing to a reduction of aspect ratio only and the limiting form of the load grading has been shown from the results given in R. & M. 2596[6] to be elliptic. Fig. 10 shows the movement towards the elliptic curve still occurring at $M = 0 \cdot 9$, and the final breakdown, which occurs in a region where the use of the Prandtl-Glauert factor is becoming untenable.

5. *Results—Tapered Wing, 28·4 deg Sweepback.*—The results for this wing were calculated by the 84-vortex lattice, before it had been demonstrated that, at this angle of sweepback, the 126-lattice would give a superior result. A further disadvantage is that the centre-line correction has not been applied. However, enough information has now been published to make possible an estimate of the errors due to both causes, and it is considered that the results still have value and can in any case be used as they stand for comparative purposes.

The results consist of 9-point standard solutions for $M = 0, 0 \cdot 6, 0 \cdot 8, 0 \cdot 9$ and $1 \cdot 0$; 9-point standard solutions for wing twist, with $c\theta$ linear, for $M = 0$ and $M = 1$; and an additional solution for $M = 1$ obtained by a 168-vortex lattice. The latter solution was included in order to verify that the solutions obtained with the revised tables have converged to the required accuracy. This step was necessary because the standard method is based on a convergence calculated from two-dimensional considerations using the bound vorticity only, and the use of the revised tables, in which the downwash is based on the trailing vorticity only, might retard the rate of convergence. As the effect is mainly chordwise, the chordwise spacing was halved to give 168 vortices, and the solutions for the 84 and 168-vortex patterns for $M = 1$ are given in Table 3, solutions 13 and 14. It will be seen that the difference in the two solutions is small at $M = 1$, and, when it is remembered that all we are concerned with is the effect on solutions for values of M below the breakdown, it is clear that effects of compressibility can be handled by the revised tables without necessity for any alteration of the lattice.

A selection of the results including load coefficient, local lift coefficient and local aerodynamic centre for $M = 0, 0 \cdot 6, 0 \cdot 8$, and $0 \cdot 9$ has been plotted in Fig. 11.

6. *Results—Triangular Wing, Aspect Ratio* 2·31.—For this wing, solutions have been calculated by the 126-vortex lattice, including the centre line correction, for $M = 0, 0 \cdot 8, 0 \cdot 9, 1 \cdot 0$. The results are given in Tables 5 and 6 and the load coefficient and local aerodynamic centre have been plotted in Fig. 12. It will be seen that the local aerodynamic centre varies less than with the other wings, and that again the load-coefficient curve tends to the elliptic until the breakdown occurs.

7. *General Discussion.*—The following results have already been demonstrated or can reasonably be deduced from the preceding sections.

(a) That the results obtained by the two methods are in good agreement at $M = 0 \cdot 8$, and should remain in agreement until beyond $M = 0 \cdot 9$, or over the useful range of application of the Prandtl-Glauert factor.

(b) That, if necessary, the auxiliary solutions to allow for the centre-line correction can be omitted and their effect estimated from solutions already published.

(c) That the curves of load coefficient of the straight and triangular wings tend to approach an elliptic curve with increase of Mach number, and that, for these wings, for which the argument can be based on decreasing aspect ratio only, the elliptic curve is probably the limit as $M \to 1$, the curves obtained in this paper at $M = 1$ being false because of the breakdown of the method which occurs between $M = 0 \cdot 9$ and $1 \cdot 0$.

(d) That, although it has been shown in R. & M. 2596[6] that, for a wide range of swept-back wings, reduction of aspect ratio with constant sweepback tends to lead to load coefficient curves which approach the elliptic, the analogy with effect of compressibility is not complete for V wings, for in the latter case the equivalent reduction of aspect ratio is accompanied by increase of sweepback to a limit of 90 deg. The limiting curve for C_K for V wings as $M \to 1$, therefore differs from the elliptic, but no prediction can now be made as to what it should be.

7.1. Some observations on conditions at $M = 1$ can now be added. Both methods break down at $M = 1$, the first because the assumption on which it is based becomes untenable, and the second because the wing area vanishes. It is interesting to note, however, that both methods still give a finite value for $dC_L/d\alpha$ at $M = 1$. For example, for the straight tapered wing, the first method gives $dC_L/d\alpha = 15 \cdot 344$. An approximate value for the second method can be deduced by lifting-line theory on the lines of work by Mr. G. H. Lee[7]. For an elliptic wing, with sectional $dC_L/d\alpha = 2\pi$, $dC_L/d\alpha$ is $2\pi A/(2 + A)$ where A is the aspect ratio. Applying the analogy that $dC_L/d\alpha$ at Mach number M is equivalent to $1/\sqrt{(1 - M^2)}$ times the value at $M = 0$, with A changed to $A\sqrt{(1 - M^2)}$, the revised value of $dC_L/d\alpha$ at M will be $2\pi A/[2 + A\sqrt{(1 - M^2)}]$. Proceeding to the limit, the ratio of $(dC_L/d\alpha)_{M=1}$ to $(dC_L/d\alpha)_{M=0}$ will be $1 + A/2$ or $3 \cdot 93$, against the value $3 \cdot 50$ (*see* Table 1) of method 1, a result which supports the conclusion that methods 1 and 2 will remain in substantial agreement until the useful limit of the Prandtl-Glauert factor has been passed.

7.2. The variations in the aerodynamic centre for the four wings have been collected together in a single table, No. 29. It will be noted that the effect on the straight wing is to give a nose-up moment with increase of M, while for the swept-back wings the effect is reversed to give a nose-down moment, which is more serious the greater the sweepback. It is possible to give a rough explanation of the observed effects which will enable the application to any given wing to be predicted. Two factors have to be taken into account (a) the alteration in spanwise load grading and (b) the change in local aerodynamic centre and for the wings treated here it seems that the latter effect is predominant. For the straight wing, the effect is almost entirely the same as a reduction in aspect ratio, which gives a general forward movement of the local aerodynamic centre leading to a nose-up moment. For the triangular wing, two effects are operative, the first being the general forward movement due to effective decrease of aspect ratio, and the second the general backward movement due to the centre-line correction, which also increases with the effective increase in sweepback which accompanies decrease of aspect ratio. For this wing the two effects practically cancel each other, leaving the aerodynamic centre almost invariable with Mach number.

For the tapered wings with sweepback, where the trailing edge has a discontinuity of slope at the centre, the backward movement due to effective increase of sweepback overcomes the forward movement due to decreasing aspect ratio, leading to curves with movement back in the centre region and forward movement in the tip region as in Fig. 11, for the moderate sweepback, and curves with a general backward movement as in Fig. 8 for the higher sweepbacks.

7.3. The influence of the change in load grading appears to be small for the wings dealt with in this report, but it should not be forgotten that there is an unexplored region of small aspect ratio and large sweepback in which load grading might assume greater importance.

Finally, it is thought that now attention has been drawn to the principles which govern the changes, it will be possible easily to predict the effects for a great variety of wing plans. It seems clear that for a conventional tapered wing, there will be a moderate angle of sweepback at which the Mach number effects on the aerodynamic centre will be negligible over a useful range of subsonic, as with the triangular wing.

8. *Conclusion.*—In conclusion, it should be added that the first method has considerable advantages in that, by preserving the plan of the wing, it is possible to compute a range of Mach numbers with very much less work than by the second method, which requires a completely independent calculation for each Mach number. In attempting to extend the work to high subsonic speeds beyond the application of the Prandtl-Glauert factor, and even to the sonic region, applications which will in the first instance depend on high speed tunnel results, it is predicted that the second method will be quite impractical.

The writer desires to acknowledge the valuable assistance rendered by Miss D. E. Lehrian in the organisation of the final stage of the work, by Miss S. D. Brown, who undertook the major part of the work of computation, and by Miss W. Tafe, who was also responsible for a small but important part of the calculations.

REFERENCES

No.	*Author*	*Title, etc.*
1	V. M. Falkner	Calculations of Compressibility effects on the Loading of a Swept-back Wing. A.R.C. 9261.
2	H. Glauert	The Effect of Compressibility on the Lift of an Aerofoil. R. & M. 1135. September, 1927.
3	A. D. Young	Note on the Effect of Compressibility on the Lift Curve Slope of a Wing of Finite Span. A.R.C. 7046. (Unpublished.)
4	V. M. Falkner	The Solution of Lifting Plane Problems by Vortex Lattice Theory. R. & M. 2591. September, 1947.
5	R. Dickson	The Relationship between the Compressible Flow round a Swept-back Aerofoil and the Incompressible Flow round Equivalent Aerofoils. A.R.C. 9986. (Unpublished.)
6	V. M. Falkner	Calculated Loadings due to Incidence of a Number of Straight and Swept-back Wings. R. & M. 2596. June, 1948.
7	G. H. Lee	Tailless Aircraft Design Problems. *Journal of the Royal Aeronautical Society.* February, 1947.

TABLE 1

Solutions for Straight Tapered Wing

1. $M = 0$: 84-vortex, 9-point standard solution: $\eta = 0\cdot2, 0\cdot5, 0\cdot8$.
2. $M = 0$: 84-vortex, 6-point standard solution: $\eta = 0\cdot2, 0\cdot5, 0\cdot8$.
3. $M = 0$: 84-vortex, 9-point standard solution for wing twist, $c\theta$ linear: $\eta = 0\cdot2, 0\cdot5, 0\cdot8$.
4. $M = 0\cdot8$: 84-vortex, 9-point standard solution.
5. $M = 0\cdot9$: 84-vortex, 9-point standard solution.
6. $M = 1\cdot0$: 84-vortex, 9-point standard solution.
7. $M = 0\cdot9$: 84-vortex, 9-point standard solution for wing twist, $c\theta$ linear.

Quantity	Solution						
	1	2	3	4	5	6	7
a_0	+ 0·08172	+ 0·08137	− 0·01121	+ 0·11364	+ 0·13617	+ 0·87269	− 0·01777
a_1	− 0·00623	− 0·00584	+ 0·00418	− 0·01417	− 0·02254	− 1·27173	0·01345
a_2	− 0·00039		0·00058	− 0·00016	+ 0·00054	− 0·13190	0·00271
c_0	− 0·02679	− 0·02544	0·04277	− 0·02207	− 0·01505	+ 1·04994	+ 0·05901
c_1	+ 0·00907	+ 0·00682	− 0·01167	+ 0·00613	− 0·00224	− 1·87069	− 0·03094
c_2	0·00204		− 0·00052	0·00391	+ 0·00452	− 1·85948	− 0·00008
e_0	0·03340	0·02931	+ 0·00061	0·03943	0·04526	+ 0·78599	+ 0·01167
e_1	− 0·02379	− 0·01760	− 0·00301	− 0·04587	− 0·06512	− 1·58397	− 0·02081
e_2	− 0·00571		− 0·00195	− 0·01763	− 0·03121	− 1·28198	− 0·01177
$dC_L/d\alpha$	4·389	4·376		6·020	7·097	15·344	
C_{Di}	1·003			1·001	1·001	1·032	
C_{m0}			− 0·0460				− 0·0754
α_0			− 0·2395				− 0·2393
a.c.	0·4788			0·4690	0·4600	− 0·0999	

Note:—Solutions are per radian incidence or per radian twist at tip.

Aerodynamic centres (a.c.) are in terms of mean chord behind apex A of Fig. 1.

C_{Di} is in terms of $(1/\pi A)\ C_L^2$.

TABLE 2

Solutions for Straight Tapered Wing

η	Solution 1. Per radian			Solution 2. Per radian		
	Load Coeff.	C_{LL}/C_L	Local a.c.	Load Coeff.	C_{LL}/C_L	Local a.c.
0	1·322	0·867	0·241	1·323	0·868	0·241
0·05	1·318	0·895	0·241			
0·10	1·311	0·923	0·241	1·313	0·924	0·241
0·15	1·298	0·948	0·241			
0·20	1·281	0·972	0·241	1·282	0·972	0·241
0·25	1·258	0·993	0·241			
0·30	1·231	1·013	0·241	1·233	1·014	0·241
0·35	1·201	1·032	0·241			
0·40	1·165	1·048	0·241	1·166	1·049	0·241
0·45	1·127	1·063	0·241			
0·50	1·083	1·074	0·241	1·084	1·075	0·241
0·55	1·037	1·085	0·241			
0·60	1·987	1·091	0·240	0·987	1·091	0·240
0·65	0·933	1·094	0·240			
0·70	0·874	1·091	0·238	0·874	1·090	0·238
0·75	0·810	1·081	0·237			
0·80	0·738	1·057	0·235	0·736	1·054	0·235
0·85	0·652	1·009	0·233			
0·90	0·548	0·921	0·229	0·544	0·915	0·230
0·95	0·398	0·784	0·227	0·396	0·780	0·227
1·00	0·000	0·706	0·223	0·000	0·699	0·223

η	Solution 3. For $C_{m0} = -0·05$			Solution 4. Per radian		
	$K/4sV$	C_{LL}	Local a.c.	Load Coeff.	C_{LL}/C_L	Local a.c.
0	− 0·0312	− 0·480	0·201	1·306	0·857	0·234
0·05	− 0·0307	− 0·491	0·200	1·304	0·885	0·234
0·10	− 0·0298	− 0·491	0·200	1·297	0·913	0·234
0·15	− 0·0280	− 0·480	0·199	1·286	0·939	0·234
0·20	− 0·0255	− 0·456	0·199	1·271	0·964	0·234
0·25	− 0·0225	− 0·418	0·197	1·251	0·988	0·233
0·30	− 0·0189	− 0·365	0·194	1·288	1·010	0·233
0·35	− 0·0147	− 0·297	0·190	1·200	1·031	0·233
0·40	− 0·0101	− 0·213	0·181	1·168	1·050	0·233
0·45	− 0·0051	− 0·113	0·153	1·132	1·068	0·232
0·50	+ 0·0002	+ 0·004	1·850	1·092	1·083	0·232
0·55	0·0056	0·138	0·258	1·048	1·095	0·230
0·60	0·0111	0·288	0·233	0·999	1·104	0·229
0·65	0·0164	0·452	0·224	0·945	1·108	0·228
0·70	0·0214	0·626	0·220	0·886	1·105	0·226
0·75	0·0257	0·805	0·217	0·820	1·093	0·223
0·80	0·0290	0·975	0·215	0·744	1·066	0·220
0·85	0·0307	1·117	0·213	0·655	1·013	0·217
0·90	0·0301	1·187	0·212	0·545	0·916	0·212
0·95	0·0250	1·157	0·211	0·394	0·775	0·207
1·00	0·000	1·164	0·210	0·000	0·688	0·202

TABLE 2—*continued*

Solutions for Straight Tapered Wing

η	Solution 5. Per radian			Solution 6. Per radian		
	Load Coeff.	C_{LL}/C_L	Local a.c.	Load Coeff.	C_{LL}/C_L	Local a.c.
0	1·299	0·852	0·227	1·139	0·747	− 0·352
0·05	1·297	0·880	0·227	1·139	0·773	− 0·351
0·10	1·291	0·908	0·227	1·139	0·801	− 0·349
0·15	1·280	0·935	0·227	1·138	0·831	− 0·345
0·20	1·266	0·960	0·226	1·138	0·863	− 0·341
0·25	1·248	0·985	0·226	1·136	0·897	− 0·335
0·30	1·225	1·009	0·226	1·134	0·933	− 0·328
0·35	1·199	1·031	0·225	1·130	0·971	− 0·321
0·40	1·169	1·051	0·224	1·124	1·011	− 0·313
0·45	1·134	1·070	0·224	1·116	1·053	− 0·306
0·50	1·095	1·086	0·222	1·104	1·095	− 0·298
0·55	1·052	1·100	0·221	1·088	1·138	− 0·290
0·60	1·004	1·110	0·219	1·067	1·179	− 0·283
0·65	0·951	1·114	0·217	1·039	1·217	− 0·277
0·70	0·891	1·112	0·214	1·001	1·249	− 0·272
0·75	0·824	1·099	0·211	0·952	1·270	− 0·268
0·80	0·747	1·070	0·207	0·888	1·272	− 0·266
0·85	0·656	1·015	0·202	0·802	1·240	− 0·266
0·90	0·545	0·915	0·197	0·683	1·148	− 0·267
0·95	0·392	0·771	0·191	0·504	0·991	− 0·270
1·00	0·000	0·681	0·184	0·000	0·896	− 0·276

η	Solution 7. For C_{m0} = − 0·05		
	$K/4sV$	C_{LL}	Local a.c.
0	− 0·0230	− 0·354	0·128
0·05	− 0·0227	− 0·363	0·128
0·10	− 0·0220	− 0·363	0·127
0·15	− 0·0207	− 0·355	0·125
0·20	− 0·0190	− 0·338	0·122
0·25	− 0·0168	− 0·311	0·118
0·30	− 0·0141	− 0·273	0·111
0·35	− 0·0111	− 0·224	0·100
0·40	− 0·0077	− 0·163	0·078
0·45	− 0·0040	− 0·090	+ 0·013
0·50	− 0·0001	− 0·003	− 3·571
0·55	+ 0·0039	+ 0·096	+ 0·282
0·60	0·0080	0·208	0·210
0·65	0·0120	0·330	0·185
0·70	0·0158	0·462	0·173
0·75	0·0191	0·597	0·165
0·80	0·0217	0·728	0·158
0·85	0·0231	0·840	0·154
0·90	0·0227	0·898	0·149
0·95	0·0190	0·880	0·146
1·00	0·0000	0·890	0·142

TABLE 3

Solutions for Tapered Wing, 28·4 deg Sweepback

8. $M = 0$: 84-vortex, 9-point standard solution: $\eta = 0 \cdot 2, 0 \cdot 5, 0 \cdot 8$.

9. $M = 0$: 84-vortex, 9-point standard solution for wing twist, $c\theta$ linear.

10. $M = 0 \cdot 6$: 84-vortex, 9-point standard solution.

11. $M = 0 \cdot 8$: 84-vortex, 9-point standard solution.

12. $M = 0 \cdot 9$: 84-vortex, 9-point standard solution.

13. $M = 1 \cdot 0$: 84-vortex, 9-point standard solution.

14. $M = 1 \cdot 0$: 168-vortex, 9-point standard solution.

15. $M = 1 \cdot 0$: 84-vortex, 9-point standard solution for wing twist, $c\theta$ linear.

Quantity	Solution							
	8	9	10	11	12	13	14	15
a_0	+ 0·07013	− 0·01017	+ 0·07542	+ 0·08093	+ 0·08518	+ 0·08586	+ 0·08695	− 0·01300
a_1	0·00423	+ 0·00291	0·01067	0·02196	0·03833	+ 0·20866	+ 0·22991	− 0·00102
a_2	0·00005	0·00010	0·00177	0·00445	0·00717	− 0·06884	− 0·06218	− 0·02327
c_0	+ 0·01766	0·02797	+ 0·03297	+ 0·05322	+ 0·07255	− 0·15051	− 0·02619	− 0·05042
c_1	− 0·03473	0·00766	− 0·05426	− 0·08061	− 0·10548	+ 0·44780	+ 0·22654	+ 0·20275
c_2	− 0·01756	0·00328	− 0·01837	− 0·01285	+ 0·00880	0·87064	+ 0·74555	+ 0·06846
e_0	+ 0·01313	+ 0·01973	+ 0·01740	+ 0·03150	+ 0·06319	+ 0·90370	+ 0·61315	+ 0·13403
e_1	− 0·00310	− 0·02717	− 0·01177	− 0·03883	− 0·09955	− 1·89273	− 1·39251	− 0·25571
e_2	+ 0·00850	− 0·00926	− 0·00476	− 0·03724	− 0·10113	− 1·23847	− 0·89470	− 0·02687
$dC_L/d\alpha$	4·285		+ 4·860	+ 5·615	+ 6·447	+ 11·805	+ 12·391	
C_{Di}	1·003		1·006	1·010	1·014	1·009	1·005	
C_{m0}		− 0·2283						− 0·5506
α_0		− 0·2268						− 0·2347
a.c.	1·068		1·076	1·086	1·095	1·175	1·169	

TABLE 4

Solutions for Tapered Wing, 28·4 deg Sweepback

η	Solution 8. Per radian			Solution 9. For $C_{m0} = -1$		
	Load Coeff.	C_{LL}/C_L	Local a.c.	$K/4sV$	C_{LL}	Local a.c.
0	1·247	0·816	0·257	− 0·120	− 1·85	0·210
0·05	1·245	0·844	0·257	− 0·119	− 1·89	0·209
0·10	1·241	0·871	0·257	− 0·115	− 1·90	0·208
0·15	1·233	0·898	0·256	− 0·109	− 1·87	0·204
0·20	1·222	0·925	0·256	− 0·100	− 1·78	0·200
0·25	1·208	0·952	0·255	− 0·089	− 1·66	0·194
0·30	1·191	0·978	0·254	− 0·076	− 1·47	0·184
0·35	1·171	1·005	0·253	− 0·061	− 1·23	0·168
0·40	1·148	1·031	0·252	− 0·044	− 0·92	0·140
0·45	1·122	1·056	0·250	− 0·025	− 0·55	+ 0·068
0·50	1·092	1·080	0·249	− 0·004	− 0·11	− 0·667
0·55	1·058	1·104	0·246	+ 0·017	+ 0·41	+ 0·465
0·60	1·020	1·124	0·244	0·039	1·01	0·324
0·65	0·976	1·142	0·241	0·061	1·67	0·282
0·70	0·927	1·153	0·238	0·082	2·40	0·260
0·75	0·869	1·156	0·235	0·101	3·17	0·246
0·80	0·799	1·142	0·231	0·117	3·93	0·235
0·85	0·714	1·102	0·227	0·127	4·60	0·226
0·90	0·603	1·020	0·223	0·126	5·04	0·218
0·95	0·442	0·931	0·218	0·107	5·33	0·211
1·00	0·000	0·822	0·213	0·000	5·36	0·204

η	Solution 10. Per radian			Solution 11. Per radian		
	Load Coeff.	C_{LL}/C_L	Local a.c.	Load Coeff.	C_{LL}/C_L	Local a.c.
0	1·229	0·804	0·264	1·212	0·792	0·274
0·05	1·228	0·832	0·264	1·210	0·819	0·274
0·10	1·224	0·859	0·263	1·207	0·847	0·273
0·15	1·217	0·887	0·262	1·202	0·875	0·272
0·20	1·208	0·914	0·262	1·194	0·903	0·270
0·25	1·196	0·942	0·260	1·184	0·932	0·268
0·30	1·182	0·970	0·259	1·172	0·961	0·265
0·35	1·164	0·998	0·257	1·157	0·991	0·262
0·40	1·144	1·026	0·254	1·139	1·022	0·259
0·45	1·120	1·054	0·252	1·118	1·052	0·255
0·50	1·093	1·082	0·249	1·095	1·083	0·251
0·55	1·063	1·108	0·246	1·067	1·112	0·246
0·60	1·027	1·132	0·243	1·035	1·140	0·241
0·65	0·986	1·153	0·239	0·997	1·165	0·236
0·70	0·939	1·169	0·235	0·952	1·184	0·230
0·75	0·883	1·174	0·231	0·898	1·194	0·224
0·80	0·815	1·164	0·226	0·832	1·187	0·218
0·85	0·730	1·126	0·222	0·747	1·152	0·212
0·90	0·617	1·045	0·217	0·634	1·072	0·206
0·95	0·453	0·956	0·212	0·467	0·983	0·200
1·00	0	0·846	0·207	0	0·872	0·195

TABLE 4—*continued*

Solutions for Tapered Wing, 28·4 deg Sweepback

η	Solution 12. Per radian			Solution 13. Per radian		
	Load Coeff.	C_{LL}/C_L	Local a.c.	Load Coeff.	C_{LL}/C_L	Local a.c.
0	1·198	0·783	0·287	1·192	0·780	0·432
0·05	1·197	0·810	0·287	1·191	0·807	0·432
0·10	1·194	0·838	0·286	1·190	0·836	0·429
0·15	1·190	0·866	0·284	1·188	0·866	0·424
0·20	1·183	0·894	0·282	1·185	0·897	0·418
0·25	1·174	0·924	0·278	1·181	0·930	0·410
0·30	1·163	0·955	0·275	1·174	0·964	0·399
0·35	1·150	0·986	0·270	1·165	0·999	0·386
0·40	1·135	1·018	0·265	1·153	1·035	0·370
0·45	1·116	1·050	0·259	1·138	1·071	0·352
0·50	1·095	1·083	0·253	1·117	1·105	0·330
0·55	1·070	1·115	0·246	1·091	1·138	0·304
0·60	1·040	1·146	0·239	1·058	1·166	0·274
0·65	1·004	1·173	0·232	1·017	1·189	0·240
0·70	0·961	1·196	0·224	0·966	1·202	0·200
0·75	0·909	1·209	0·216	0·903	1·202	0·154
0·80	0·844	1·205	0·208	0·826	1·180	0·101
0·85	0·760	1·172	0·200	0·729	1·125	+ 0·041
0·90	0·646	1·093	0·192	0·605	1·024	− 0·029
0·95	0·477	1·005	0·184	0·434	0·913	− 0·109
1·00	0·000	0·894	0·176	0·000	0·784	− 0·202

η	Solution 14. Per radian			Solution 15. For $C_{m_0} = -1$		
	Load Coeff.	C_{LL}/C_L	Local a.c.	$K/4sV$	C_{LL}	Local a.c.
0	1·205	0·789	0·431	− 0·077	− 1·19	0·044
0·05	1·205	0·816	0·430	− 0·076	− 1·22	0·039
0·10	1·204	0·846	0·427	− 0·074	− 1·22	+ 0·023
0·15	1·203	0·876	0·422	− 0·070	− 1·20	− 0·004
0·20	1·201	0·908	0·415	− 0·064	− 1·14	− 0·047
0·25	1·197	0·942	0·406	− 0·057	− 1·06	− 0·111
0·30	1·191	0·978	0·394	− 0·049	− 0·94	− 0·206
0·35	1·182	1·013	0·381	− 0·038	− 0·77	− 0·365
0·40	1·169	1·049	0·365	− 0·027	− 0·58	− 0·660
0·45	1·152	1·084	0·346	− 0·015	− 0·33	− 1·451
0·50	1·130	1·118	0·325	− 0·002	− 0·04	− 13·371
0·55	1·100	1·147	0·301	+ 0·012	+ 0·29	+ 2·375
0·60	1·063	1·171	0·273	0·026	0·67	1·157
0·65	1·015	1·187	0·241	0·040	1·09	0·773
0·70	0·958	1·192	0·204	0·053	1·54	0·570
0·75	0·887	1·180	0·162	0·065	2·02	0·435
0·80	0·801	1·144	0·114	0·074	2·49	0·333
0·85	0·696	1·074	+ 0·056	0·080	2·90	0·249
0·90	0·567	0·960	− 0·011	0·079	3·15	0·175
0·95	0·397	0·836	− 0·092	0·067	3·32	0·107
1·00	0·000	0·696	− 0·190	0·000	3·32	0·043

TABLE 5

Solutions for Delta Wing

16. $M = 0$: 126-vortex, 8-point solution.

17. $M = 0 \cdot 8$: 126-vortex, 8-point solution.

18. $M = 0 \cdot 9$: 126-vortex, 8-point solution.

19. $M = 1 \cdot 0$: 126-vortex, 8-point solution.

Quantity	Solution			
	16	17	18	19
a_0	+ 0·10493	+ 0·10959	+ 0·11087	− 0·02407
a_1	0·02111	0·02358	0·03080	0·41249
c_0	+ 0·04263	+ 0·03755	+ 0·04149	+ 0·37902
c_1	− 0·10884	− 0·07947	− 0·07572	− 0·67474
e_0	− 0·05158	− 0·03310	− 0·02856	− 0·17785
e_1	+ 0·06931	+ 0·03861	+ 0·02726	+ 0·23605
p_0	− 0·21402	− 0·20065	− 0·20509	− 0·30418
p_1	+ 0·42804	+ 0·40130	+ 0·41018	+ 0·60837
$dC_L/d\alpha$	2·517	2·715	2·856	4·219
C_{Di}	1·010	1·002	1·001	1·002
a.c.	1·185	1·193	1·204	1·441

TABLE 6

Solutions for Delta Wing

η	Solution 16. Per radian			Solution 17. Per radian		
	Load Coeff.	C_{LL}/C_L	Local a.c.	Load Coeff.	C_{LL}/C_L	Local a.c.
0	1·332	0·666	0·355	1·298	0·649	0·348
0·05	1·330	0·700	0·348	1·296	0·682	0·341
0·10	1·324	0·735	0·336	1·291	0·717	0·330
0·15	1·313	0·773	0·325	1·282	0·754	0·322
0·20	1·299	0·812	0·316	1·270	0·794	0·314
0·25	1·280	0·854	0·309	1·254	0·836	0·308
0·30	1·257	0·898	0·303	1·235	0·882	0·303
0·35	1·229	0·945	0·297	1·211	0·931	0·298
0·40	1·916	0·997	0·291	1·182	0·985	0·293
0·45	1·157	1·052	0·285	1·149	1·045	0·288
0·50	1·113	1·113	0·280	1·111	1·111	0·284
0·55	1·063	1·181	0·274	1·067	1·185	0·279
0·60	1·006	1·257	0·269	1·016	1·270	0·275
0·65	0·942	1·345	0·264	0·959	1·369	0·271
0·70	0·870	1·450	0·259	0·893	1·489	0·267
0·75	0·789	1·579	0·255	0·819	1·637	0·263
0·80	0·699	1·747	0·251	0·733	1·833	0·259
0·85	0·596	1·987	0·249	0·634	2·114	0·256
0·90	0·477	2·383	0·248	0·515	2·576	0·253
0·95	0·328	3·278	0·248	0·361	3·610	0·251
1·00	0	—	0·250	0	—	0·250

η	Solution 18. Per radian			Solution 19. Per radian		
	Load Coeff.	C_{LL}/C_L	Local a.c.	Load Coeff.	C_{LL}/C_L	Local a.c.
0	1·283	0·642	0·353	1·253	0·627	0·607
0·05	1·281	0·674	0·346	1·252	0·659	0·600
0·10	1·277	0·709	0·336	1·250	0·694	0·585
0·15	1·269	0·747	0·327	1·245	0·732	0·571
0·20	1·258	0·786	0·320	1·238	0·774	0·555
0·25	1·244	0·829	0·314	1·229	0·819	0·540
0·30	1·226	0·876	0·309	1·217	0·869	0·523
0·35	1·204	0·926	0·304	1·201	0·924	0·506
0·40	1·178	0·981	0·299	1·181	0·984	0·487
0·45	1·147	1·043	0·295	1–156	1·051	0·468
0·50	1·111	1·111	0·290	1·125	1·125	0·448
0·55	1·069	1·188	0·286	1·088	1·208	0·427
0·60	1·021	1·277	0·281	1·042	1·303	0·406
0·65	0·966	1·380	0·277	0·988	1·412	0·385
0·70	0·903	1·505	0·272	0·925	1·541	0·364
0·75	0·830	1·661	0·268	0·849	1·699	0·343
0·80	0·747	1·866	0·264	0·761	1·902	0·323
0·85	0·648	2·160	0·260	0·656	2·187	0·303
0·90	0·529	2·644	0·257	0·530	2·649	0·285
0·95	0·372	3·723	0·253	0·367	3·673	0·267
1·00	0	—	0·250	0	—	0·250

TABLE 7

Solution 20: 59 deg Tapered Wing:
$M = 0$: 84-*Vortex*, 3-*Point Standard Solution for Incidence:*
$\eta = 0\cdot2,\ 0\cdot5,\ 0\cdot8$

a_0	$0\cdot07171$	$dC_L/d\alpha = 2\cdot610$	
c_0	$0\cdot01222$	Local a.c. $0\cdot25$ chord.	
e_0	$0\cdot00625$		

η	C_{LL}/C_L	$C_{LL}c/C_L\bar{c}$
0	0·755	1·208
0·1	0·814	1·204
0·2	0·877	1·192
0·3	0·945	1·171
0·4	1·018	1·140
0·5	1·097	1·097
0·6	1·179	1·037
0·7	1·254	0·953
0·8	1·297	0·830
0·9	1·211	0·630
0·95	1·005	0·462
1·00	0	0

To convert solution to $M = 0\cdot8$ for 45 deg wing, multiply $dC_L/d\alpha$ by $1\cdot\dot{6}$.

TABLE 8

Solution 21: 59 deg Tapered Wing:
$M = 0$: 84-*vortex*, 6-*Point Standard Solution for Incidence:*
$\eta = 0\cdot2,\ 0\cdot5,\ 0\cdot8$

a_0	$0\cdot06458$	c_0	$0\cdot03087$	e_0	$0\cdot00916$
a_1	$0\cdot01525$	c_1	$-0\cdot03241$	e_1	$-0\cdot01401$
$dC_L/d\alpha$	$2\cdot630$				

η	C_{LL}/C_L	$C_{LL}c/C_L\bar{c}$	Local a.c.
0	0·755	1·207	0·276
0·1	0·813	1·204	0·276
0·2	0·877	1·193	0·274
0·3	0·946	1·173	0·271
0·4	1·021	1·143	0·266
0·5	1·101	1·101	0·260
0·6	1·182	1·040	0·253
0·7	1·256	0·954	0·244
0·8	1·292	0·827	0·233
0·9	1·198	0·623	0·220
0·95	0·990	0·455	0·214
1·00	0·000	0·000	0·206

To convert solution to $M = 0\cdot8$ for 45 deg wing, multiply $dC_L/d\alpha$ by $1\cdot\dot{6}$

TABLE 9

Solution 22: 59 deg Tapered Wing:
$M = 0$: 84-Vortex, 9-Point Standard Solution for Incidence:
$\eta = 0 \cdot 2,\ 0 \cdot 5,\ 0 \cdot 8$

a_0	0·06414	c_0	0·10277	e_0	0·01668
a_1	0·01754	c_1	− 0·14162	e_1	− 0·00284
a_2	0·00256	c_2	− 0·10079	e_2	− 0·01720

$dC_L/d\alpha = 2 \cdot 860$ a.c. $= 1 \cdot 746\bar{c}$ behind apex.

η	C_{LL}/C_L	$C_{LL}c/C_L\bar{c}$	Local a.c.
0	0·701	1·121	0·276
0·05	0·728	1·121	0·275
0·10	0·757	1·120	0·275
0·15	0·788	1·119	0·274
0·20	0·822	1·118	0·272
0·25	0·858	1·116	0·271
0·30	0·898	1·113	0·269
0·35	0·941	1·110	0·266
0·40	0·987	1·105	0·264
0·45	1·036	1·099	0·261
0·50	1·090	1·090	0·259
0·55	1·147	1·078	0·256
0·60	1·208	1·063	0·253
0·65	1·270	1·042	0·250
0·70	1·333	1·013	0·248
0·75	1·391	0·974	0·246
0·80	1·436	0·919	0·243
0·85	1·452	0·842	0·242
0·90	1·402	0·729	0·240
0·95	1·192	0·548	0·239
1·00	0	0	0·238

To convert solution to $M = 0 \cdot 8$ for 45 deg wing, multiply $dC_L/d\alpha$ by $1 \cdot \dot{6}$

TABLE 10

Solution 23: 59 deg Tapered Wing:
$M = 0$: 84-Vortex, 12-Point Standard Solution for Incidence:
Reduced by Least Squares: $\eta = 0 \cdot 2,\ 0 \cdot 5,\ 0 \cdot 7,\ 0 \cdot 8$

a_0	0·06194	c_0	0·11360	e_0	− 0·00127
a_1	0·01201	c_1	− 0·11752	e_1	− 0·01632
a_2	0·01210	c_2	− 0·19905	e_2	0·11477

$dC_L/d\alpha = 2 \cdot 780$

η	C_{LL}/C_L	$C_{LL}c/C_L\bar{c}$	Local a.c.
0	0·672	1·075	0·250
0·1	0·728	1·078	0·251
0·2	0·799	1·087	0·255
0·3	0·886	1·099	0·261
0·4	0·990	1·109	0·266
0·5	1·111	1·111	0·269
0·6	1·244	1·094	0·268
0·7	1·376	1·046	0·261
0·8	1·471	0·941	0·248
0·9	1·408	0·732	0·226
0·95	1·179	0·542	0·212
1·00	0	0	0·195

To convert solution to $M = 0 \cdot 8$ for 45 deg. wing multiply $dC_L/d\alpha$ by $1 \cdot \dot{6}$

(22975)

TABLE 11

Solution 24: 59 deg Tapered Wing:

$M = 0$: 126-Vortex, 3-Point Standard Solution for Incidence:

$\eta = 0 \cdot 2,\ 0 \cdot 6,\ 0 \cdot 8$

a_0	0·07177	$dC_L/d\alpha$ = 2·585	
c_0	0·00276	Local a.c. 0·25 chord.	
e_0	0·01905		

η	C_{LL}/C_L	$C_{LL}c/C_L\bar{c}$
0	0·763	1·221
0·1	0·821	1·215
0·2	0·881	1·199
0·3	0·944	1·171
0·4	1·012	1·134
0·5	1·085	1·085
0·6	1·164	1·024
0·7	1·242	0·944
0·8	1·297	0·830
0·9	1·234	0·642
0·95	1·037	0·477
1·0	0	0

To convert solution to $M = 0 \cdot 8$ for 45 deg wing, multiply $dC_L/d\alpha$ by $1 \cdot \dot{6}$

TABLE 12

Solution 25: 59 deg Tapered Wing:

$M = 0$: 126-Vortex, 6-Point Standard Solution for Incidence:

$\eta = 0 \cdot 2,\ 0 \cdot 6,\ 0 \cdot 8$

a_0	0·06536	c_0	0·01317	e_0	0·02986
a_1	0·01700	c_1	− 0·02266	e_1	− 0·02285
$dC_L/d\alpha$ = 2·647		a.c. 1·692$\bar{c}$ behind apex.			

η	C_{LL}/C_L	$C_{LL}c/C_L\bar{c}$	Local a.c.
0	0·767	1·227	0·279
0·05	0·796	1·226	0·279
0·10	0·825	1·222	0·278
0·15	0·855	1·214	0·278
0·20	0·885	1·204	0·277
0·25	0·916	1·191	0·276
0·30	0·948	1·176	0·275
0·35	0·981	1·157	0·273
0·40	1·015	1·136	0·271
0·45	1·050	1·113	0·269
0·50	1·086	1·086	0·266
0·55	1·124	1·056	0·263
0·60	1·162	1·022	0·260
0·65	1·200	0·984	0·255
0·70	1·236	0·940	0·251
0·75	1·267	0·887	0·245
0·80	1·286	0·823	0·240
0·85	1·280	0·742	0·233
0·90	1·218	0·633	0·227
0·95	1·021	0·470	0·220
1·00	0	0	0·212

To convert solution to $M = 0 \cdot 8$ for 45 deg wing, multiply $dC_L/d\alpha$ by $1 \cdot \dot{6}$

TABLE 13

Solution 26: 59 deg Tapered Wing:

$M = 0$: 126-*Vortex*, 9-*Point Standard Solution for Incidence:*

$\eta = 0{\cdot}2,\ 0{\cdot}6,\ 0{\cdot}8$

a_0	$0{\cdot}06578$	c_0	$-0{\cdot}01439$	e_0	$0{\cdot}08223$
a_1	$0{\cdot}01642$	c_1	$0{\cdot}02333$	e_1	$-0{\cdot}11095$
a_2	$-0{\cdot}00128$	c_2	$0{\cdot}04204$	e_2	$-0{\cdot}07743$

$dC_L/d\alpha = 2{\cdot}648$ a.c. $1{\cdot}695\ \bar{c}$ behind apex.

η	C_{LL}/C_L	$C_{LL}c/C_L\bar{c}$	Local a.c.
0	0·768	1·229	0·280
0·05	0·797	1·227	0·280
0·10	0·826	1·222	0·280
0·15	0·855	1·214	0·279
0·20	0·885	1·203	0·279
0·25	0·914	1·189	0·278
0·30	0·945	1·172	0·277
0·35	0·977	1·152	0·275
0·40	1·009	1·130	0·273
0·45	1·043	1·106	0·271
0·50	1·079	1·078	0·268
0·55	1·116	1·049	0·265
0·60	1·155	1·016	0·261
0·65	1·195	0·980	0·256
0·70	1·234	0·938	0·251
0·75	1·270	0·889	0·245
0·80	1·295	0·829	0·238
0·85	1·297	0·752	0·231
0·90	1·244	0·647	0·223
0·95	1·052	0·484	0·214
1·00	0	0	0·206

To convert solution to $M = 0{\cdot}8$ for 45 deg wing, multiply $dC_L/d\alpha$ by $1{\cdot}\dot{6}$

TABLE 14

Solution 27: 59 deg Tapered Wing:

$M = 0$: 126-*Vortex*, 6-*Point Standard Solution Corrected by Auxiliary Solution at* $\eta = 0,\ 0{\cdot}2$

a_0'	$0{\cdot}03004$	p_0	$-0{\cdot}36434$
a_1'	$-0{\cdot}05207$	p_1	$0{\cdot}59181$

$P = 0{\cdot}65P_a + 0{\cdot}35P_b$ $dC_L/d\alpha = 2{\cdot}582$

a.c. $1{\cdot}736\bar{c}$ behind apex.

η	C_{LL}/C_L	$C_{LL}c/C_L\bar{c}$	Local a.c.
0	0·700	1·119	0·383
0·05	0·737	1·135	0·364
0·10	0·784	1·160	0·334
0·15	0·828	1·176	0·312
0·20	0·870	1·183	0·294
0·25	0·909	1·182	0·282
0·30	0·948	1·175	0·275
0·35	0·986	1·164	0·273
0·40	1·025	1·148	0·271
0·45	1·065	1·129	0·269
0·50	1·106	1·106	0·266
0·55	1·148	1·079	0·263
0·60	1·190	1·047	0·260
0·65	1·232	1·010	0·255
0·70	1·272	0·967	0·251
0·75	1·306	0·914	0·245
0·80	1·328	0·850	0·240
0·85	1·323	0·768	0·233
0·90	1·260	0·655	0·227
0·95	1·058	0·486	0·220
1·00	0·000	0·000	0·212

To convert solution to $M = 0{\cdot}8$ for 45 deg wing, multiply $dC_L/d\alpha$ by $1{\cdot}\dot{6}$

TABLE 15

Solution 28: 59 deg Tapered Wing:
$M = 0$: 126-Vortex, 6-Point Standard Solution for Wing Twist, θ Linear, $\eta = 0{\cdot}2,\ 0{\cdot}6,\ 0{\cdot}8$

a_0	$-0{\cdot}01429$	c_0	$0{\cdot}04843$	e_0	$0{\cdot}00012$
a_1	$0{\cdot}00443$	c_1	$0{\cdot}01478$	e_1	$-0{\cdot}03030$
α_0	$-0{\cdot}3745$	C_{m0}	$-0{\cdot}3132$		

η	C_{LL} for $C_{m0} = -1$	$K/4sV$ for $C_{m0} = -1$ at $M = 0{\cdot}8$	Local a.c.
0	− 1·060	− 0·0727	0·204
0·05	− 1·087	− 0·0717	0·203
0·10	− 1·088	− 0·0690	0·200
0·15	− 1·059	− 0·0645	0·195
0·20	− 0·998	− 0·0582	0·187
0·25	− 0·905	− 0·0504	0·174
0·30	− 0·775	− 0·0412	0·154
0·35	− 0·609	− 0·0308	0·117
0·40	− 0·406	− 0·0195	+ 0·037
0·45	− 0·166	− 0·0075	− 0·304
0·50	+ 0·114	+ 0·0049	+ 1·083
0·55	0·427	0·0172	0·475
0·60	0·774	0·0292	0·371
0·65	1·147	0·0403	0·325
0·70	1·540	0·0501	0·297
0·75	1·934	0·0580	0·277
0·80	2·301	0·0631	0·261
0·85	2·603	0·0647	0·246
0·90	2·740	0·0611	0·231
0·95	2·486	0·0490	0·217
1·00	0	0	0·202

To convert solution to $M = 0{\cdot}8$ for 45 deg wing, multiply C_{m0} by $1{\cdot}\dot{6}$

TABLE 16

Solution 29: 59 deg Tapered Wing:
$M = 0$: 126-Vortex, 6-Point Standard Solution for Wing Twist, θ Linear, Corrected by Auxiliary Solution: $\eta = 0,\ 0{\cdot}1$

a_0'	$-0{\cdot}00166$	p_{a0}	$0{\cdot}04379$	p_{b0}	$-0{\cdot}01080$
a_1'	$0{\cdot}00710$	p_{a1}	$-0{\cdot}08871$	p_{b1}	$-0{\cdot}00766$
α_0	$-0{\cdot}3573$	C_{m0}	$-0{\cdot}3261$		

η	C_{LL} for $C_{m0} = -1$	$K/4sV$ for $C_{m0} = -1$ at $M = 0{\cdot}8$	Local a.c.
0	− 1·164	− 0·0798	0·277
0·05	− 1·180	− 0·0779	0·263
0·10	− 1·156	− 0·0733	0·237
0·15	− 1·093	− 0·0665	0·218
0·20	− 1·002	− 0·0584	0·199
0·25	− 0·889	− 0·0495	0·176
0·30	− 0·745	− 0·0396	0·154
0·35	− 0·572	− 0·0289	0·117
0·40	− 0·362	− 0·0174	+ 0·037
0·45	− 0·120	− 0·0054	− 0·304
0·50	+ 0·160	+ 0·0069	+ 1·083
0·55	0·472	0·0190	0·475
0·60	0·814	0·0307	0·371
0·65	1·183	0·0416	0·325
0·70	1·566	0·0510	0·297
0·75	1·952	0·0586	0·277
0·80	2·309	0·0634	0·261
0·85	2·602	0·0647	0·246
0·90	2·731	0·0609	0·231
0·95	2·469	0·0487	0·217
1·00	0·000	0·0000	0·202

To convert solution to $M = 0{\cdot}8$, for 45 deg wing, multiply C_{m0} by $1{\cdot}\dot{6}$

TABLE 17

Solution 30: 45 deg Tapered Wing:
$M = 0$: 126-Vortex, 6-Point Standard Solution for Incidence:
$\eta = 0{\cdot}2,\ 0{\cdot}6,\ 0{\cdot}8$

a_0	0·06004	c_0	— 0·00268	e_0	0·03132
a_1	0·00686	c_1	— 0·00686	e_1	— 0·02732

$dC_L/d\alpha = 3{\cdot}672$ a.c. $1{\cdot}656\bar{c}$ behind apex.

η	C_{LL}/C_L	$C_{LL}c/C_L\bar{c}$	Local a.c.
0	0·787	1·260	0·264
0·05	0·817	1·258	0·264
0·10	0·846	1·252	0·263
0·15	0·876	1·243	0·263
0·20	0·904	1·230	0·263
0·25	0·934	1·214	0·262
0·30	0·963	1·194	0·262
0·35	0·993	1·171	0·261
0·40	1·022	1·145	0·260
0·45	1·052	1·116	0·259
0·50	1·084	1·084	0·257
0·55	1·115	1·048	0·254
0·60	1·147	1·009	0·252
0·65	1·178	0·966	0·248
0·70	1·207	0·917	0·244
0·75	1·230	0·861	0·239
0·80	1·244	0·796	0·234
0·85	1·231	0·714	0·227
0·90	1·167	0·607	0·220
0·95	0·974	0·448	0·213
1·00	0	0	0·204

TABLE 18

Solution 31: 45 deg Tapered Wing:
$M = 0$: 126-Vortex, 9-Point Standard Solution for Incidence:
$\eta = 0{\cdot}2,\ 0{\cdot}6,\ 0{\cdot}8$

a_0	0·06104	c_0	— 0·01508	e_0	0·06017
a_1	0·00536	c_1	0·01403	e_1	— 0·07508
a_2	— 0·00135	c_2	0·01724	e_2	— 0·03866

$dC_L/d\alpha = 3{\cdot}694$ a.c. $1{\cdot}659\bar{c}$ behind apex.

η	C_{LL}/C_L	$C_{LL}c/C_L\bar{c}$	Local a.c.
0	0·786	1·157	0·263
0·05	0·815	1·255	0·263
0·10	0·844	1·249	0·263
0·15	0·873	1·240	0·263
0·20	0·902	1·226	0·263
0·25	0·930	1·209	0·263
0·30	0·959	1·189	0·262
0·35	0·988	1·166	0·261
0·40	1·017	1·139	0·260
0·45	1·047	1·110	0·259
0·50	1·078	1·078	0·257
0·55	1·110	1·044	0·255
0·60	1·144	1·006	0·252
0·65	1·176	0·965	0·248
0·70	1·209	0·919	0·243
0·75	1·237	0·866	0·238
0·80	1·255	0·803	0·231
0·85	1·249	0·724	0·224
0·90	1·192	0·620	0·216
0·95	1·002	0·461	0·207
1·00	0	0	0·197

TABLE 19

Solution 32: 45 deg Tapered Wing:
$M = 0$: 126-*Vortex*, 6-*Point Standard Solution for Incidence:*
Modified by Auxiliary Solution: $\eta = 0,\ 0{\cdot}2$

a_0'	$0{\cdot}02303$	p_0	$-\ 0{\cdot}26723$
a_1'	$-\ 0{\cdot}04040$	p_1	$0{\cdot}43754$
$dC_L/d\alpha =$	$3{\cdot}596$	a.c. =	$1{\cdot}692\bar{c}$ behind apex.

η	C_{LL}/C_L	$C_{LL}c/C_L\bar{c}$	Local a.c.
0	0·731	1·169	0·346
0·05	0·768	1·182	0·330
0·10	0·812	1·202	0·306
0·15	0·853	1·211	0·287
0·20	0·892	1·213	0·273
0·25	0·928	1·206	0·262
0·30	0·963	1·194	0·262
0·35	0·997	1·177	0·261
0·40	1·031	1·155	0·260
0·45	1·066	1·130	0·259
0·50	1·100	1·100	0·257
0·55	1·135	1·067	0·254
0·60	1·171	1·030	0·252
0·65	1·205	0·988	0·248
0·70	1·237	0·940	0·244
0·75	1·263	0·884	0·239
0·80	1·278	0·818	0·234
0·85	1·266	0·735	0·227
0·90	1·202	0·625	0·220
0·95	1·004	0·462	0·213
1·00	0	0	0·204

TABLE 20

Solution 33: 45 deg Tapered Wing:
$M = 0$: 126-*Vortex*, 6-*Point Standard Solution for Twist,*
θ *Linear:* $\eta = 0{\cdot}2,\ 0{\cdot}6,\ 0{\cdot}8$

a_0	$-\ 0{\cdot}01249$	c_0	$0{\cdot}04801$	e_0	$-\ 0{\cdot}00539$
a_1	$0{\cdot}00311$	c_1	$0{\cdot}00861$	e_1	$-\ 0{\cdot}02348$
α_0	$-\ 0{\cdot}38201$	C_{m0}	$-\ 0{\cdot}4500$		

η	C_{LL} for $C_{m0} = -\ 1$	$K/4sV$ for $C_{m0} = -\ 1$	Local a.c.
0	− 1·107	− 0·0764	0·214
0·05	− 1·135	− 0·0753	0·214
0·10	− 1·135	− 0·0724	0·212
0·15	− 1·102	− 0·0674	0·208
0·20	− 1·036	− 0·0607	0·202
0·25	− 0·933	− 0·0523	0·193
0·30	− 0·793	− 0·0424	0·178
0·35	− 0·615	− 0·0313	0·150
0·40	− 0·399	− 0·0193	+ 0·088
0·45	− 0·144	− 0·0066	− 0·213
0·50	+ 0·151	+ 0·0065	+ 0·691
0·55	0·477	0·0193	0·384
0·60	0·836	0·0317	0·320
0·65	1·216	0·0430	0·289
0·70	1·611	0·0528	0·270
0·75	2·001	0·0604	0·255
0·80	2·357	0·0650	0·242
0·85	2·636	0·0659	0·230
0·90	2·742	0·0614	0·217
0·95	2·454	0·0487	0·204
1·00	0	0	0·189

TABLE 21

Solution 34: 45 deg Tapered Wing:
$M = 0$: *126-Vortex, 6-Point Standard Solution for Twist, θ Linear, Corrected by Auxiliary Solution,* $\eta = 0,\ 0\cdot1$, *and* $0\cdot2$

a_0'	$-\ 0\cdot00034$	p_{a0}	$0\cdot03725$	p_{b0}	$-\ 0\cdot01774$
a_1'	$0\cdot00448$	p_{a1}	$-\ 0\cdot07762$	p_{b1}	$0\cdot00705$
α_0	$-\ 0\cdot3680$	C_{m0}	$-\ 0\cdot4751$		

η	C_{LL} for $C_{m0} = -1$	$K/4sV$ for $C_{m0} = -1$	Local a.c.
0	− 1·218	− 0·0840	0·268
0·05	− 1·231	− 0·0817	0·256
0·10	− 1·200	− 0·0766	0·235
0·15	− 1·130	− 0·0692	0·221
0·20	− 1·030	− 0·0604	0·207
0·25	− 0·906	− 0·0508	0·193
0·30	− 0·752	− 0·0402	0·178
0·35	− 0·567	− 0·0288	0·150
0·40	− 0·347	− 0·0167	+ 0·088
0·45	− 0·091	− 0·0042	− 0·213
0·50	+ 0·201	+ 0·0087	+ 0·691
0·55	0·522	0·0212	0·384
0·60	0·872	0·0331	0·320
0·65	1·244	0·0440	0·289
0·70	1·627	0·0533	0·270
0·75	2·003	0·0604	0·255
0·80	2·348	0·0647	0·242
0·85	2·613	0·0653	0·230
0·90	2·710	0·0607	0·217
0·95	2·418	0·0479	0·024
1·00	0	0	0·189

TABLE 22

Solution 35: 45 deg Tapered Wing:
$M = 0\cdot8$: *126-Vortex, 6-Point Standard Solution for Incidence:* $\eta = 0\cdot2,\ 0\cdot6,\ 0\cdot8$

a_0	$0\cdot06705$	c_0	$0\cdot00805$	e_0	$0\cdot04228$
a_1	$0\cdot01593$	c_1	$-\ 0\cdot00795$	e_1	$-\ 0\cdot05046$

$dC_L/d\alpha = 4\cdot475$ a.c. $1\cdot687\bar{c}$ behind apex.

η	C_{LL}/C_L	$C_{LL}c/C_L\bar{c}$	Local a.c.
0	0·764	1·222	0·277
0·05	0·793	1·220	0·276
0·10	0·822	1·217	0·276
0·15	0·852	1·210	0·276
0·20	0·882	1·200	0·276
0·25	0·914	1·188	0·275
0·30	0·946	1·173	0·274
0·35	0·980	1·156	0·273
0·40	1·014	1·136	0·272
0·45	1·050	1·113	0·270
0·50	1·088	1·088	0·268
0·55	1·126	1·059	0·264
0·60	1·166	1·026	0·260
0·65	1·204	0·988	0·256
0·70	1·242	0·943	0·250
0·75	1·273	0·891	0·243
0·80	1·293	0·827	0·236
0·85	1·285	0·745	0·227
0·90	1·223	0·636	0·217
0·95	1·023	0·471	0·206
1·00	0	0	0·195

TABLE 23

Solution 36: 45 deg Tapered Wing:
M = 0·8: 126-Vortex, 9-Point Standard Solution for
Incidence: η = 0·2, 0·6, 0·8

a_0	0·06838	c_0	− 0·02865	e_0	0·11192
a_1	0·01398	c_1	0·05380	e_1	− 0·16826
a_2	− 0·00264	c_2	0·05608	e_2	− 0·10289

$dC_L/d\alpha = 4·489$ a.c. $1·691\bar{c}$ behind apex.

η	C_{LL}/C_L	$C_{LL}c/C_L\bar{c}$	Local a.c.
0	0·765	1·224	0·278
0·05	0·794	1·222	0·278
0·10	0·823	1·218	0·278
0·15	0·852	1·210	0·277
0·20	0·881	1·199	0·277
0·25	0·912	1·185	0·277
0·30	0·942	1·169	0·276
0·35	0·974	1·150	0·275
0·40	1·007	1·128	0·274
0·45	1·042	1·104	0·272
0·50	1·078	1·078	0·270
0·55	1·116	1·050	0·266
0·60	1·157	1·018	0·262
0·65	1·198	0·982	0·256
0·70	1·239	0·941	0·250
0·75	1·276	0·893	0·242
0·80	1·304	0·834	0·233
0·85	1·307	0·758	0·223
0·90	1·256	0·653	0·212
0·95	1·063	0·489	0·200
1·00	0	0	0·187

TABLE 24

Solution 37: 45 deg Tapered Wing:
M = 0·8: 126-Vortex, 6-Point Standard Solution for
Incidence: Modified by Auxiliary Solution: η = 0, 0·2

a_0'	0·03142	p_0	− 0·38003
a_1'	− 0·05517	p_1	0·62850

$dC_L/d\alpha = 4·372$ a.c. $1·731\bar{c}$ behind apex.

η	C_{LL}/C_L	$C_{LL}c/C_L\bar{c}$	Local a.c.
0	0·700	1·120	0·385
0·05	0·737	1·135	0·366
0·10	0·783	1·159	0·334
0·15	0·826	1·173	0·312
0·20	0·868	1·180	0·294
0·25	0·907	1·179	0·282
0·30	0·946	1·173	0·274
0·35	0·985	1·162	0·273
0·40	1·024	1·147	0·272
0·45	1·064	1·129	0·270
0·50	1·106	1·106	0·268
0·55	1·149	1·080	0·264
0·60	1·192	1·049	0·260
0·65	1·234	1·012	0·256
0·70	1·275	0·969	0·250
0·75	1·309	0·917	0·243
0·80	1·332	0·852	0·236
0·85	1·326	0·769	0·227
0·90	1·263	0·656	0·217
0·95	1·058	0·486	0·206
1·00	0	0	0·195

TABLE 25

Solution 38: 45 deg Tapered Wing:
$M = 0{\cdot}8$: 126-Vortex, 6-Point Standard Solution for Wing Twist, θ Linear: $\eta = 0{\cdot}2,\ 0{\cdot}6,\ 0{\cdot}8$

a_0	$-0{\cdot}01451$	c_0	$0{\cdot}04753$	e_0	$0{\cdot}00340$
a_1	$0{\cdot}00452$	c_1	$0{\cdot}01841$	e_1	$-0{\cdot}03781$
α_0	$-0{\cdot}3754$	C_{m0}	$-0{\cdot}5232$		

η	C_{LL} for $C_{m0} = -1$	$K/4sV$ for $C_{m0} = -1$	Local a.c.
0	− 1·066	− 0·0736	0·204
0·05	− 1·093	− 0·0726	0·203
0·10	− 1·094	− 0·0698	0·200
0·15	− 1·065	− 0·0652	0·194
0·20	− 1·004	− 0·0588	0·185
0·25	− 0·910	− 0·0510	0·171
0·30	− 0·778	− 0·0416	0·149
0·35	− 0·612	− 0·0311	0·110
0·40	− 0·407	− 0·0196	+ 0·023
0·45	− 0·164	− 0·0075	− 0·348
0·50	+ 0·116	+ 0·0050	+ 1·132
0·55	0·431	0·0175	0·488
0·60	0·780	0·0296	0·377
0·65	1·155	0·0408	0·328
0·70	1·547	0·0507	0·297
0·75	1·942	0·0586	0·275
0·80	2·312	0·0638	0·256
0·85	2·613	0·0653	0·238
0·90	2·750	0·0616	0·222
0·95	2·490	0·0494	0·204
1·00	0	0	0·186

TABLE 26

Solution 39: 45 deg Tapered Wing:
$M = 0{\cdot}8$: 126-Vortex, 6-Point Standard Solution for Wing Twist, θ Linear, Modified by Auxiliary Solution: $\eta = 0,\ 0{\cdot}1,\ 0{\cdot}2$

a_0'	$-0{\cdot}00149$	p_{a0}	$0{\cdot}04721$	p_{b0}	$-0{\cdot}01368$
a_1'	$0{\cdot}00673$	p_{a1}	$-0{\cdot}09673$	p_{b1}	$-0{\cdot}00095$
α_0	$-0{\cdot}35857$	C_{m0}	$-0{\cdot}5454$		

η	C_{LL} for $C_{m0} = -1$	$K/4sV$ for $C_{m0} = -1$	Local a.c.
0	− 1·167	− 0·0805	0·275
0·05	− 1·183	− 0·0785	0·260
0·10	− 1·157	− 0·0738	0·234
0·15	− 1·096	− 0·0671	0·215
0·20	− 1·004	− 0·0589	0·196
0·25	− 0·891	− 0·0499	0·173
0·30	− 0·748	− 0·0400	0·149
0·35	− 0·573	− 0·0291	0·110
0·40	− 0·363	− 0·0175	+ 0·023
0·45	− 0·118	− 0·0054	− 0·348
0·50	+ 0·160	+ 0·0069	+ 1·132
0·55	0·473	0·0192	0·488
0·60	0·819	0·0310	0·377
0·65	1·186	0·0419	0·328
0·70	1·570	0·0514	0·297
0·75	1·956	0·0590	0·275
0·80	2·316	0·0639	0·256
0·85	2·606	0·0651	0·238
0·90	2·736	0·0613	0·222
0·95	2·470	0·0490	0·204
1·00	0	0	0·186

TABLE 27

Solution 40: 45 *deg Tapered Wing:*

$M = 1$: 126-*Vortex,* 6-*Point Standard Solution for Wing Twist;* θ *Linear:*

$\eta = 0\cdot2,\ 0\cdot6,\ 0\cdot8$

a_0	$-0\cdot02028$	c_0	$0\cdot03849$	e_0	$0\cdot03103$
a_1	$0\cdot00994$	c_1	$0\cdot05523$	e_1	$-0\cdot08151$
α_0	$-0\cdot36074$	C_{m0}	$-0\cdot7339$		

η	C_{LL} for $C_{m0} = -1$	$K/4sV$ for $C_{m0} = -1$	Local a.c.
0	− 0·950	− 0·0655	0·169
0·05	− 0·975	− 0·0647	0·167
0·10	− 0·978	− 0·0624	0·161
0·15	− 0·956	− 0·0585	0·149
0·20	− 0·907	− 0·0532	0·132
0·25	− 0·830	− 0·0465	0·104
0·30	− 0·721	− 0·0385	+ 0·061
0·35	− 0·580	− 0·0295	− 0·013
0·40	− 0·405	− 0·0196	− 0·168
0·45	− 0·195	− 0·0089	− 0·706
0·50	+ 0·053	+ 0·0023	+ 4·061
0·55	0·335	0·0136	0·882
0·60	0·652	0·0247	0·584
0·65	1·001	0·0354	0·465
0·70	1·376	0·0451	0·398
0·75	1·765	0·0532	0·351
0·80	2·144	0·0591	0·315
0·85	2·469	0·0617	0·283
0·90	2·654	0·0595	0·255
0·95	2·457	0·0487	0·227
1·00	0	0	0·200

TABLE 28

Results for 45 deg Tapered Wing at $M = 0 \cdot 8$

by Two Methods Based on the Prandtl-Glauert Factor

Wing	Incidence				Wing twist: θ linear		
	Soln.	$dC_L/d\alpha$	$dC_L/d\alpha$ for 45° wing	a.c.	C_{m0}	C_{m0} for 45° wing	α_0
45 deg : $M = 0$	32		3·596	1·692			
	34					− 0·475	− 0·368
45 deg : $M = 0 \cdot 8$ first method	37		4·372	1·731			
	39					− 0·545	− 0·359
59 deg : $M = 0$ equivalent to 45 deg : $M = 0 \cdot 8$ second method	27	2·582	4·303	1·736			
	29				− 0·326	− 0·544	− 0·357

TABLE 29

Variation of Aerodynamic Centre with Mach Number for Four Wings

The Aerodynamic Centre is given in Terms of $\bar{c}$ behind the Apex at the Centre Section

M	Straight tapered wing	Tapered wing 28·4 deg sweepback	Triangular wing	45 deg tapered wing
0	0·479	1·068	1·185	1·692
0·6	—	1·076	—	—
0·8	0·469	1·086	1·193	1·736
0·9	0·460	1·095	1·204	—

TABLE 30

Induced Downwash Factors. $y = 0$

x	F		Δ	x	F		Δ
	x +ve	x −ve			x +ve	x −ve	
0	2·0000	2·0000	999	1·8	0·2517	3·7483	215
0·05	1·9001	2·0999	991	1·9	0·2302	3·7698	191
0·10	1·8010	2·1990	977	2·0	0·2111	3·7889	318
0·15	1·7033	2·2967	955	2·2	0·1793	3·8207	255
0·20	1·6078	2·3922	929	2·4	0·1538	3·8462	205
0·25	1·5149	2·4851	896	2·6	0·1333	3·8667	168
0·30	1·4253	2·5747	860	2·8	0·1165	3·8835	139
0·35	1·3393	2·6607	821	3·0	0·1026	3·8974	116
0·40	1·2572	2·7428	779	3·2	0·0910	3·9090	97
0·45	1·1793	2·8207	737	3·4	0·0813	3·9187	83
0·50	1·1056	2·8944	694	3·6	0·0730	3·9270	71
0·55	1·0362	2·9638	652	3·8	0·0659	3·9341	62
0·60	0·9710	3·0290	610	4·0	0·0597	3·9403	121
0·65	0·9100	3·0900	569	4·5	0·0476	3·9524	88
0·70	0·8531	3·1469	531	5·0	0·0388	3·9612	65
0·75	0·8000	3·2000	494	5·5	0·0323	3·9677	51
0·80	0·7506	3·2494	459	6	0·0272	3·9728	71
0·85	0·7047	3·2953	426	7	0·0201	3·9799	47
0·90	0·6621	3·3379	396	8	0·0154	3·9846	32
0·95	0·6225	3·3775	367	9	0·0122	3·9878	23
1·00	0·5858	3·4142	341	10	0·0099	3·9901	55
1·05	0·5517	3·4483	316	15	0·0044	3·9956	19
1·10	0·5201	3·4799	293	20	0·0025	3·9975	9
1·15	0·4908	3·5092	272	25	0·0016	3·9984	5
1·20	0·4636	3·5364	253	30	0·0011	3·9989	3
1·25	0·4383	3·5617	235	35	0·0008	3·9992	2
1·30	0·4148	3·5852	219	40	0·0006	3·9994	1
1·35	0·3929	3·6071	204	45	0·0005	3·9995	1
1·40	0·3725	3·6275	366	50	0·0004	3·9996	1
1·5	0·3359	3·6641	319	60	0·0003	3·9997	1
1·6	0·3040	3·6960	279	80	0·0002	3·9998	2
1·7	0·2761	3·7239	244	100	0	4·0000	

TABLE 31

Induced Downwash Factors. $y = 2$

x	F		Δ	x	F		Δ
	x +ve	x −ve			x +ve	x −ve	
0	− 0·6666	− 0·6667	884	3·4	0·0428	− 1·3761	20
0·1	− 0·5782	− 0·7551	855	3·6	0·0408	− 1·3741	20
0·2	− 0·4927	− 0·8406	802	3·8	0·0388	− 1·3721	20
0·3	− 0·4125	− 0·9208	732	4·0	0·0368	− 1·3701	19
0·4	− 0·3393	− 0·9940	651	4·2	0·0349	− 1·3682	27
0·5	− 0·2742	− 1·0591	567	4·5	0·0322	− 1·3655	41
0·6	− 0·2175	− 1·1158	486	5·0	0·0281	− 1·3614	35
0·7	− 0·1689	− 1·1644	411	5·5	0·0246	− 1·3579	30
0·8	− 0·1278	− 1·2055	343	6·0	0·0216	− 1·3549	25
0·9	− 0·0935	− 1·2398	286	6·5	0·0191	− 1·3524	22
1·0	− 0·0649	− 1·2684	235	7	0·0169	− 1·3502	34
1·1	− 0·0414	− 1·2919	192	8	0·0135	− 1·3468	25
1·2	− 0·0222	− 1·3111	157	9	0·0110	− 1·3443	19
1·3	− 0·0065	− 1·3268	126	10	0·0091	− 1·3424	14
1·4	0·0061	− 1·3394	102	11	0·0077	− 1·3410	34
1·5	0·0163	− 1·3496	82	15	0·0043	− 1·3376	18
1·6	0·0245	− 1·3578	65	20	0·0025	− 1·3358	9
1·7	0·0310	− 1·3643	50	25	0·0016	− 1·3349	5
1·8	0·0360	− 1·3693	69	30	0·0011	− 1·3344	3
2·0	0·0429	− 1·3762	37	35	0·0008	− 1·3341	2
2·2	0·0466	− 1·3799	16	40	0·0006	− 1·3339	1
2·4	0·0482	− 1·3815	2	45	0·0005	− 1·3338	1
2·6	0·0484	− 1·3817	7	50	0·0004	− 1·3337	1
2·8	0·0477	− 1·3810	14	60	0·0003	− 1·3336	1
3·0	0·0463	− 1·3796	16	80	0·0002	− 1·3335	1
3·2	0·0447	− 1·3780	19	100	0·0001	− 1·3334	

TABLE 32

Induced Downwash Factors. $y = 4$ *and* 6

x	F for $y = 4$		Δ
	x +ve	x −ve	
0·0	− 0·1334	− 0·1333	142
0·2	− 0·1192	− 0·1475	139
0·4	− 0·1053	− 0·1614	135
0·6	− 0·0918	− 0·1749	127
0·8	− 0·0791	− 0·1876	119
1·0	− 0·0672	− 0·1995	110
1·2	− 0·0562	− 0·2105	99
1·4	− 0·0463	− 0·2204	88
1·6	− 0·0375	− 0·2292	79
1·8	− 0·0296	− 0·2371	69
2·0	− 0·0227	− 0·2440	59
2·2	− 0·0168	− 0·2499	51
2·4	− 0·0117	− 0·2550	44
2·6	− 0·0073	− 0·2594	37
2·8	− 0·0036	− 0·2631	30
3·0	− 0·0006	− 0·2661	26
3·2	0·0020	− 0·2687	21
3·4	0·0041	− 0·2708	17
3·6	0·0058	− 0·2725	14
3·8	0·0072	− 0·2739	12
4·0	0·0084	− 0·2751	18
4·5	0·0102	− 0·2769	8
5·0	0·0110	− 0·2777	3
5·5	0·0113	− 0·2780	2
6	0·0111	− 0·2778	8
7	0·0103	− 0·2770	12
8	0·0091	− 0·2758	11
9	0·0080	− 0·2747	10
10	0·0070	− 0·2737	32
15	0·0038	− 0·2705	15
20	0·0023	− 0·2690	8
25	0·0015	− 0·2682	4
30	0·0011	− 0·2678	3
35	0·0008	− 0·2675	2
40	0·0006	− 0·2673	1
45	0·0005	− 0·2672	1
50	0·0004	− 0·2671	2
60	0·0002	− 0·2669	1
80	0·0001	− 0·2668	0
100	0·0001	− 0·2668	

x	F for $y = 6$		Δ
	x +ve	x −ve	
0·0	− 0·0572	− 0·0571	98
0·5	− 0·0474	− 0·0669	93
1·0	− 0·0381	− 0·0762	85
1·5	− 0·0296	− 0·0847	75
2·0	− 0·0221	− 0·0922	63
2·5	− 0·0158	− 0·0985	53
3·0	− 0·0105	− 0·1038	41
3·5	− 0·0064	− 0·1079	33
4·0	− 0·0031	− 0·1112	25
4·5	− 0·0006	− 0·1137	18
5·0	0·0012	− 0·1155	14
5·5	0·0026	− 0·1169	9
6·0	0·0035	− 0·1178	11
7·0	0·0046	− 0·1189	3
8·0	0·0049	− 0·1192	2
10·0	0·0047	− 0·1190	16
15·0	0·0031	− 0·1174	11
20	0·0020	− 0·1163	6
25	0·0014	− 0·1157	4
30	0·0010	− 0·1153	3
35	0·0007	− 0·1150	1
40	0·0006	− 0·1149	1
45	0·0005	− 0·1148	1
50	0·0004	− 0·1147	1
60	0·0003	− 0·1146	1
80	0·0002	− 0·1145	1
100	0·0001	− 0·1144	

TABLE 33

Induced Downwash Factors. $y = 8(2)14$

x	F for $y = 8$		Δ	x	F for $y = 12$		Δ
	x +ve	x −ve			x +ve	x −ve	
0	− 0·0318	− 0·0317	80	0	− 0·0140	− 0·0140	46
1	− 0·0238	− 0·0397	72	2	− 0·0094	− 0·0186	38
2	− 0·0166	− 0·0469	60	4	− 0·0056	− 0·0224	29
3	− 0·0106	− 0·0529	46	6	− 0·0027	− 0·0253	19
4	− 0·0060	− 0·0575	33	8	− 0·0008	− 0·0272	11
5	− 0·0027	− 0·0608	23	10	0·0003	− 0·0283	9
6	− 0·0004	− 0·0631	14	15	0·0012	− 0·0292	0
7	0·0010	− 0·0645	9	20	0·0012	− 0·0292	3
8	0·0019	− 0·0654	8	25	0·0009	− 0·0289	1
10	0·0027	− 0·0662	3	30	0·0008	− 0·0288	2
15	0·0024	− 0·0659	6	35	0·0006	− 0·0286	1
20	0·0018	− 0·0653	5	40	0·0005	− 0·0285	1
25	0·0013	− 0·0648	4	45	0·0004	− 0·0284	0
30	0·0009	− 0·0644	2	50	0·0004	− 0·0284	2
35	0·0007	− 0·0642	1	60	0·0002	− 0·0282	1
40	0·0006	− 0·0641	1	80	0·0001	− 0·0281	0
45	0·0005	− 0·0640	1	100	0·0001	− 0·0281	
50	0·0004	− 0·0639	1				
60	0·0003	− 0·0638	2				
80	0·0001	− 0·0636	0				
100	0·0001	− 0·0636					
	F for $y = 10$				F for $y = 14$		
0	− 0·0202	− 0·0202	78	0	− 0·0103	− 0·0102	29
2	− 0·0124	− 0·0280	63	2	− 0·0074	− 0·0131	26
4	− 0·0061	− 0·0343	40	4	− 0·0048	− 0·0157	20
6	− 0·0021	− 0·0383	23	6	− 0·0028	− 0·0177	15
8	0·0002	− 0·0406	10	8	− 0·0013	− 0·0192	9
10	0·0012	− 0·0416	6	10	− 0·0004	− 0·0201	11
15	0·0018	− 0·0422	3	15	0·0007	− 0·0212	3
20	0·0015	− 0·0419	4	20	0·0010	− 0·0215	2
25	0·0011	− 0·0415	2	25	0·0008	− 0·0213	1
30	0·0009	− 0·0413	2	30	0·0007	− 0·0212	1
35	0·0007	− 0·0411	2	35	0·0006	− 0·0211	1
40	0·0005	− 0·0409	1	40	0·0005	− 0·0210	1
45	0·0004	− 0·0408	0	45	0·0004	− 0·0209	1
50	0·0004	− 0·0408	1	50	0·0003	− 0·0208	0
60	0·0003	− 0·0407	1	60	0·0003	− 0·0208	1
80	0·0002	− 0·0406	1	80	0·0002	− 0·0207	1
100	0·0001	− 0·0405		100	0·0001	− 0·0206	

TABLE 34

Induced Downwash Factors. $y = 16(2)22$

x	F for $y = 16$		Δ	x	F for $y = 20$		Δ
	x +ve	x −ve			x +ve	x −ve	
0	− 0·0078	− 0·0079	20	0	− 0·0050	− 0·0050	10
2	− 0·0058	− 0·0099	17	2	− 0·0040	− 0·0060	9
4	− 0·0041	− 0·0116	14	4	− 0·0031	− 0·0069	8
6	− 0·0027	− 0·0130	12	6	− 0·0023	− 0·0077	7
8	− 0·0015	− 0·0142	8	8	− 0·0016	− 0·0084	6
10	− 0·0007	− 0·0150	10	10	− 0·0010	− 0·0090	9
15	0·0003	− 0·0160	4	15	− 0·0001	− 0·0099	4
20	0·0007	− 0·0164	0	20	0·0003	− 0·0103	2
25	0·0007	− 0·0164	1	25	0·0005	− 0·0105	0
30	0·0006	− 0·0163	1	30	0·0005	− 0·0105	1
35	0·0005	− 0·0162	1	40	0·0004	− 0·0104	1
40	0·0004	− 0·0161	0	50	0·0003	− 0·0103	1
45	0·0004	− 0·0161	1	60	0·0002	− 0·0102	0
50	0·0003	− 0·0160	1	80	0·0002	− 0·0102	1
60	0·0002	− 0·0159	1	100	0·0001	− 0·0101	
80	0·0001	− 0·0158	0				
100	0·0001	− 0·0158					

	F for $y = 18$				F for $y = 22$		
0	− 0·0062	− 0·0062	14	0	− 0·0041	− 0·0042	17
2	− 0·0048	− 0·0076	13	5	− 0·0024	− 0·0059	14
4	− 0·0035	− 0·0089	11	10	− 0·0010	− 0·0073	8
6	− 0·0024	− 0·0100	8	15	− 0·0002	− 0·0081	3
8	− 0·0016	− 0·0108	7	20	0·0001	− 0·0084	2
10	− 0·0009	− 0·0115	10	25	0·0003	− 0·0086	0
15	0·0001	− 0·0125	4	30	0·0003	− 0·0086	0
20	0·0005	− 0·0129	0	40	0·0003	− 0·0086	1
25	0·0005	− 0·0129	0	50	0·0002	− 0·0085	1
30	0·0005	− 0·0129	1	100	0·0001	− 0·0084	
35	0·0004	− 0·0128	0				
40	0·0004	− 0·0128	1				
45	0·0003	− 0·0127	0				
50	0·0003	− 0·0127	1				
60	0·0002	− 0·0126	1				
80	0·0001	− 0·0125	0				
100	0·0001	− 0·0125					

TABLE 35

Induced Downwash Factors. $y = 24(2)38$

x	F for $y = 24$		Δ	x	F for $y = 32$		Δ
	x +ve	x −ve			x +ve	x −ve	
0	− 0·0035	− 0·0035	14	0	− 0·0020	− 0·0019	7
5	− 0·0021	− 0·0049	10	5	− 0·0013	− 0·0026	4
10	− 0·0011	− 0·0059	8	10	− 0·0009	− 0·0030	4
15	− 0·0003	− 0·0067	3	15	− 0·0005	− 0·0034	3
20	0·0000	− 0·0070	2	20	− 0·0002	− 0·0037	2
25	0·0002	− 0·0072	1	25	0·0000	− 0·0039	1
30	0·0003	− 0·0073	0	30	0·0001	− 0·0040	1
40	0·0003	− 0·0073	1	40	0·0002	− 0·0041	0
50	0·0002	− 0·0072	1	50	0·0002	− 0·0041	1
100	0·0001	− 0·0071		100	0·0001	− 0·0040	
	F for $y = 26$				F for $y = 34$		
0	− 0·0030	− 0·0029	11	0	− 0·0017	− 0·0018	4
5	− 0·0019	− 0·0040	9	5	− 0·0013	− 0·0022	4
10	− 0·0010	− 0·0049	6	10	− 0·0009	− 0·0026	4
15	− 0·0004	− 0·0055	4	15	− 0·0005	− 0·0030	3
20	0·0000	− 0·0059	2	20	− 0·0002	− 0·0033	1
25	0·0002	− 0·0061	1	25	− 0·0001	− 0·0034	1
30	0·0003	− 0·0062	0	30	0·0000	− 0·0035	1
40	0·0003	− 0·0062	1	40	0·0001	− 0·0036	0
50	0·0002	− 0·0061	1	50	0·0001	− 0·0036	0
100	0·0001	− 0·0060		100	0·0001	− 0·0036	
	F for $y = 28$				F for $y = 36$		
0	− 0·0026	− 0·0025	9	0	− 0·0015	− 0·0016	4
5	− 0·0017	− 0·0034	8	5	− 0·0011	− 0·0020	4
10	− 0·0009	− 0·0042	5	10	− 0·0007	− 0·0024	2
15	− 0·0004	− 0·0047	3	15	− 0·0005	− 0·0026	3
20	− 0·0001	− 0·0050	2	20	− 0·0002	− 0·0029	1
25	0·0001	− 0·0052	1	25	− 0·0001	− 0·0030	1
30	0·0002	− 0·0053	0	30	0·0000	− 0·0031	1
40	0·0002	− 0·0053	0	40	0·0001	− 0·0032	0
50	0·0002	− 0·0053	1	50	0·0001	− 0·0032	0
100	0·0001	− 0·0052		100	0·0001	− 0·0032	
	F for $y = 30$				F for $y = 38$		
0	− 0·0022	− 0·0022	8	0	− 0·0014	− 0·0014	4
5	− 0·0014	− 0·0030	5	5	− 0·0010	− 0·0018	3
10	− 0·0009	− 0·0035	5	10	− 0·0007	− 0·0021	2
15	− 0·0004	− 0·0040	3	15	− 0·0005	− 0·0023	2
20	− 0·0001	− 0·0043	2	20	− 0·0003	− 0·0025	2
25	0·0001	− 0·0045	1	25	− 0·0001	− 0·0027	1
30	0·0002	− 0·0046	0	30	0·0000	− 0·0028	1
40	0·0002	− 0·0046	0	40	0·0001	− 0·0029	0
50	0·0002	− 0·0046	1	50	0·0001	− 0·0029	0
100	0·0001	− 0·0045		100	0·0001	− 0·0029	

TABLE 36

Induced Downwash Factors. $y = 40(2)58$ . .

x	F for $y = 40$		Δ	x	F for $y = 50$		Δ
	x +ve	x −ve			x +ve	x −ve	
0	− 0·0013	− 0·0012	6	0	− 0·0008	− 0·0008	2
10	− 0·0007	− 0·0018	5	10	− 0·0006	− 0·0010	4
20	− 0·0002	− 0·0023	2	20	− 0·0002	− 0·0014	1
30	0·0000	− 0·0025	1	30	− 0·0001	− 0·0015	1
40	0·0001	− 0·0026	0	40	0·0000	− 0·0016	0
50	0·0001	− 0·0026	0	50	0·0000	− 0·0016	1
100	0·0001	− 0·0026		100	0·0001	− 0·0017	
	F for $y = 42$				F for $y = 52$		
0	− 0·0012	− 0·0011	5	0	− 0·0008	− 0·0007	3
10	− 0·0007	− 0·0016	5	10	− 0·0005	− 0·0010	2
20	− 0·0002	− 0·0021	1	20	− 0·0003	− 0·0012	2
30	− 0·0001	− 0·0022	1	30	− 0·0001	− 0·0014	1
40	0·0000	− 0·0023	1	40	0·0000	− 0·0015	0
50	0·0001	− 0·0024	0	50	0·0000	− 0·0015	1
100	0·0001	− 0·0024		100	0·0001	− 0·0016	
	F for $y = 44$				F for $y = 54$		
0	− 0·0011	− 0·0010	5	0	− 0·0007	− 0·0007	3
10	− 0·0006	− 0·0015	4	10	− 0·0004	− 0·0010	2
20	− 0·0002	− 0·0019	1	20	− 0·0002	− 0·0012	1
30	− 0·0001	− 0·0020	1	30	− 0·0001	− 0·0013	1
40	0·0000	− 0·0021	1	40	0·0000	− 0·0014	0
50	0·0001	− 0·0022	0	50	0·0000	− 0·0014	1
100	0·0001	− 0·0022		100	0·0001	− 0·0015	
	F for $y = 46$				F for $y = 56$		
0	− 0·0010	− 0·0009	5	0	− 0·0007	− 0·0006	3
10	− 0·0005	− 0·0014	2	10	− 0·0004	− 0·0009	2
20	− 0·0003	− 0·0016	2	20	− 0·0002	− 0·0011	1
30	− 0·0001	− 0·0018	1	30	− 0·0001	− 0·0012	1
40	0·0000	− 0·0019	1	40	0·0000	− 0·0013	0
50	0·0001	− 0·0020	0	50	0·0000	− 0·0013	1
100	0·0001	− 0·0020		100	0·0001	− 0·0014	
	F for $y = 48$				F for $y = 58$		
0	− 0·0008	− 0·0009	3	0	− 0·0006	− 0·0006	2
10	− 0·0005	− 0·0012	3	10	− 0·0004	− 0·0008	2
20	− 0·0002	− 0·0015	2	20	− 0·0002	− 0·0010	1
30	0·0000	− 0·0017	1	30	− 0·0001	− 0·0011	1
40	0·0001	− 0·0018	0	40	0	− 0·0012	0
50	0·0001	− 0·0018	0	50	0	− 0·0012	0
100	0·0001	− 0·0018		100	0	− 0·0012	

TABLE 37

Induced Downwash Factors. $y = 60(2)74$

x	F for $y = 60$: x +ve	F for $y = 60$: x −ve	Δ
0	− 0·0005	− 0·0006	1
10	− 0·0004	− 0·0007	2
20	− 0·0002	− 0·0009	1
30	− 0·0001	− 0·0010	1
40	0	− 0·0011	0
50	0	− 0·0011	0
100	0	− 0·0011	

x	F for $y = 62$: x +ve	F for $y = 62$: x −ve	Δ
0	− 0·0005	− 0·0005	1
10	− 0·0004	− 0·0006	1
20	− 0·0003	− 0·0007	2
30	− 0·0001	− 0·0009	1
40	0	− 0·0010	0
50	0	− 0·0010	0
100	0	− 0·0010	

x	F for $y = 64$: x +ve	F for $y = 64$: x −ve	Δ
0	− 0·0005	− 0·0005	2
10	− 0·0003	− 0·0007	1
20	− 0·0002	− 0·0008	1
30	− 0·0001	− 0·0009	0
40	− 0·0001	− 0·0009	1
50	0	− 0·0010	0
100	0	− 0·0010	

x	F for $y = 66$: x +ve	F for $y = 66$: x −ve	Δ
0	− 0·0004	− 0·0005	1
10	− 0·0003	− 0·0006	1
20	− 0·0002	− 0·0007	1
30	− 0·0001	− 0·0008	1
40	0	− 0·0009	0
50	0	− 0·0009	0
100	0	− 0·0009	

x	F for $y = 68$: x +ve	F for $y = 68$: x −ve	Δ
0	− 0·0005	− 0·0004	2
10	− 0·0003	− 0·0006	1
20	− 0·0002	− 0·0007	1
30	− 0·0001	− 0·0008	0
40	− 0·0001	− 0·0008	1
50	0	− 0·0009	0
100	0	− 0·0009	

x	F for $y = 70$: x +ve	F for $y = 70$: x −ve	Δ
0	− 0·0004	− 0·0004	1
10	− 0·0003	− 0·0005	1
20	− 0·0002	− 0·0006	1
30	− 0·0001	− 0·0007	1
40	0	− 0·0008	0
50	0	− 0·0008	0
100	0	− 0·0008	

x	F for $y = 72$: x +ve	F for $y = 72$: x −ve	Δ
0	− 0·0004	− 0·0004	1
10	− 0·0003	− 0·0005	1
20	− 0·0002	− 0·0006	1
30	− 0·0001	− 0·0007	0
40	− 0·0001	− 0·0007	1
50	0	− 0·0008	0
100	0	− 0·0008	

x	F for $y = 74$: x +ve	F for $y = 74$: x −ve	Δ
0	− 0·0003	− 0·0004	0
10	− 0·0003	− 0·0004	1
20	− 0·0002	− 0·0005	1
30	− 0·0001	− 0·0006	1
40	0	− 0·0007	0
50	0	− 0·0007	0
100	0	− 0·0007	

TABLE 38

Induced Downwash Factors. $y = 13(8)45$

$\frac{1}{4}x$	$4F$ for $y = 13$		Δ
	x +ve	x −ve	
0·0	− 0·0476	− 0·0476	59
0·2	− 0·0417	− 0·0535	57
0·4	− 0·0360	− 0·0592	55
0·6	− 0·0305	− 0·0647	51
0·8	− 0·0254	− 0·0698	47
1·0	− 0·0207	− 0·0745	43
1·2	− 0·0164	− 0·0788	37
1·4	− 0·0127	− 0·0825	32
1·6	− 0·0095	− 0·0857	27
1·8	− 0·0068	− 0·0884	24
2·0	− 0·0044	− 0·0908	66
3·0	0·0022	− 0·0974	19
4·0	0·0041	− 0·0993	1
5·0	0·0042	− 0·0994	4
6·0	0·0038	− 0·0990	5
7·0	0·0033	− 0·0985	5
8·0	0·0028	− 0·0980	8
10·0	0·0020	− 0·0972	6
12·5	0·0014	− 0·0966	4
15	0·0010	− 0·0962	4
20	0·0006	− 0·0958	2
25	0·0004	− 0·0956	1
30	0·0003	− 0·0955	1
40	0·0002	− 0·0954	1
60	0·0001	− 0·0953	1
100	0	− 0·0952	

$\frac{1}{4}x$	$4F$ for $y = 21$		Δ
0·0	− 0·0182	− 0·0182	34
0·5	− 0·0148	− 0·0216	33
1·0	− 0·0115	− 0·0249	29
1·5	− 0·0086	− 0·0278	25
2	− 0·0061	− 0·0303	37
3	− 0·0024	− 0·0340	22
4	− 0·0002	− 0·0362	11
5	0·0009	− 0·0373	5
6	0·0014	− 0·0378	2
8	0·0016	− 0·0380	2
10	0·0014	− 0·0378	6
15	0·0008	− 0·0372	3
20	0·0005	− 0·0369	2
25	0·0003	− 0·0367	0
30	0·0003	− 0·0367	1
40	0·0002	− 0·0366	1
60	0·0001	− 0·0365	1
100	0	− 0·0364	

$\frac{1}{4}x$	$4F$ for $y = 29$		Δ
	x +ve	x −ve	
0·0	− 0·0095	− 0·0095	13
0·5	− 0·0082	− 0·0108	13
1	− 0·0069	− 0·0121	23
2	− 0·0046	− 0·0144	33
4	− 0·0013	− 0·0177	15
6	0·0002	− 0·0192	6
8	0·0008	− 0·0198	1
10	0·0009	− 0·0199	2
15	0·0007	− 0·0197	2
20	0·0005	− 0·0195	1
25	0·0004	− 0·0194	2
30	0·0002	− 0·0192	1
40	0·0001	− 0·0191	0
60	0·0001	− 0·0191	1
100	0	− 0·0190	

$\frac{1}{4}x$	$4F$ for $y = 37$		Δ
0	− 0·0059	− 0·0058	13
1	− 0·0046	− 0·0071	12
2	− 0·0034	− 0·0083	18
4	− 0·0016	− 0·0101	12
6	− 0·0004	− 0·0113	6
8	0·0002	− 0·0119	2
10	0·0004	− 0·0121	1
15	0·0005	− 0·0122	1
20	0·0004	− 0·0121	1
25	0·0003	− 0·0120	1
30	0·0002	− 0·0119	1
50	0·0001	− 0·0118	1
100	0	− 0·0117	

$\frac{1}{4}x$	$4F$ for $y = 45$		Δ
0	− 0·0039	− 0·0040	29
5	− 0·0010	− 0·0069	11
10	0·0001	− 0·0080	3
15	0·0004	− 0·0083	1
20	0·0003	− 0·0082	0
25	0·0003	− 0·0082	1
30	0·0002	− 0·0081	1
50	0·0001	− 0·0080	1
100	0	− 0·0079	

TABLE 39

Induced Downwash Factors. $y = 53(8)125$

$\frac{1}{4}x$	4F for y = 53		Δ
	x +ve	x −ve	
0	− 0·0028	− 0·0029	28
10	0·0000	− 0·0057	3
20	0·0003	− 0·0060	1
30	0·0002	− 0·0059	1
50	0·0001	− 0·0058	1
100	0	− 0·0057	

$\frac{1}{4}x$	4F for y = 61		Δ
0	− 0·0021	− 0·0022	20
10	− 0·0001	− 0·0042	3
20	0·0002	− 0·0045	0
25	0·0002	− 0·0045	0
30	0·0002	− 0·0045	1
50	0·0001	− 0·0044	1
100	0	− 0·0043	

$\frac{1}{4}x$	4F for y = 69		Δ
0	− 0·0017	− 0·0017	15
10	− 0·0002	− 0·0032	3
20	0·0001	− 0·0035	0
30	0·0001	− 0·0035	0
50	0·0001	− 0·0035	1
100	0	− 0·0034	

$\frac{1}{4}x$	4F for y = 77		Δ
0	− 0·0014	− 0·0013	12
10	− 0·0002	− 0·0025	3
20	0·0001	− 0·0028	0
25	0·0001	− 0·0028	0
30	0·0001	− 0·0028	0
50	0·0001	− 0·0028	1
100	0	− 0·0027	

$\frac{1}{4}x$	4F for y = 85		Δ
0	− 0·0011	− 0·0011	9
10	− 0·0002	− 0·0020	3
20	0·0001	− 0·0023	0
30	0·0001	− 0·0023	0
50	0·0001	− 0·0023	1
100	0	− 0·0022	

$\frac{1}{4}x$	4F for y = 93		Δ
	x +ve	x −ve	
0	− 0·0010	− 0·0009	7
10	− 0·0003	− 0·0016	3
20	0·0000	− 0·0019	0
25	0·0000	− 0·0019	1
30	0·0001	− 0·0020	0
50	0·0001	− 0·0020	1
100	0	− 0·0019	

$\frac{1}{4}x$	4F for y = 101		Δ
0	− 0·0008	− 0·0008	5
10	− 0·0003	− 0·0013	3
20	0·0000	− 0·0016	1
30	0·0001	− 0·0017	0
50	0·0001	− 0·0017	1
100	0	− 0·0016	

$\frac{1}{4}x$	4F for y = 109		Δ
0	− 0·0006	− 0·0007	4
10	− 0·0002	− 0·0011	2
20	0·0000	− 0·0013	1
25	0·0001	− 0·0014	0
30	0·0001	− 0·0014	0
50	0·0001	− 0·0014	1
100	0	− 0·0013	

$\frac{1}{4}x$	4F for y = 117		Δ
0	− 0·0006	− 0·0006	4
10	− 0·0002	− 0·0010	2
20	− 0·0000	− 0·0012	0
30	0·0000	− 0·0012	1
50	0·0001	− 0·0013	1
100	0	− 0·0012	

$\frac{1}{4}x$	4F for y = 125		Δ
0	− 0·0005	− 0·0005	3
10	− 0·0002	− 0·0008	2
20	0	− 0·0010	0
25	0	− 0·0010	0
30	0	− 0·0010	0
50	0	− 0·0010	0
100	0	− 0·0010	

TABLE 40

Induced Downwash Factors. $y = 133(8)141(16)173$

$\frac{1}{4}x$	4F for y = 133, x +ve	4F for y = 133, x −ve	Δ
0	− 0·0005	− 0·0004	3
10	− 0·0002	− 0·0007	2
20	0	− 0·0009	0
30	0	− 0·0009	0
50	0	− 0·0009	0
100	0	− 0·0009	
	4F for y = 141		
0	− 0·0004	− 0·0004	2
10	− 0·0002	− 0·0006	2
20	0	− 0·0008	0
25	0	− 0·0008	0
30	0	− 0·0008	0
50	0	− 0·0008	0
100	0	− 0·0008	
	4F for y = 157		
0	− 0·0003	− 0·0003	1
10	− 0·0002	− 0·0004	1
20	0·0001	− 0·0005	1
30	0	− 0·0006	0
50	0	− 0·0006	0
100	0	− 0·0006	
	4F for y = 173		
0	− 0·0002	− 0·0003	1
10	− 0·0001	− 0·0004	1
20	0	− 0·0005	0
25	0	− 0·0005	0
30	0	− 0·0005	0
50	0	− 0·0005	0
100	0	− 0·0005	

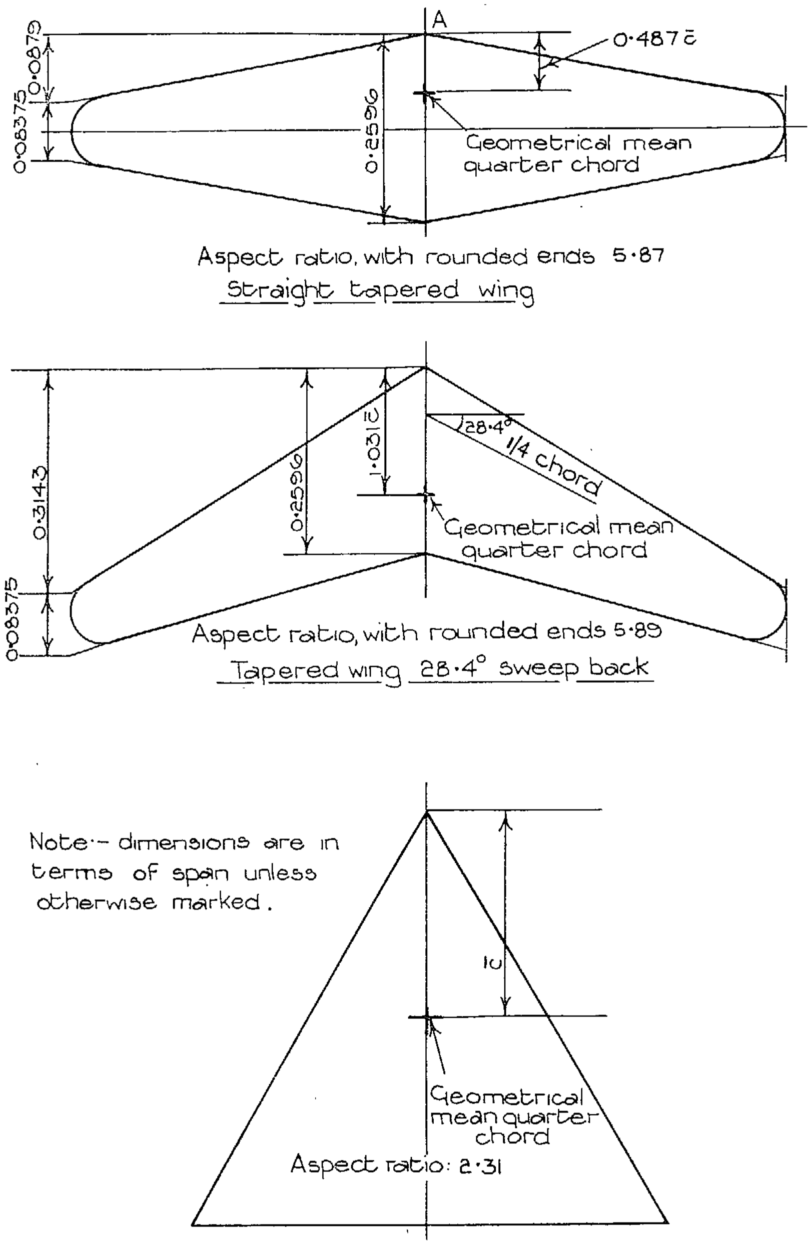

FIG. 1. Delta wing: equilateral triangle.

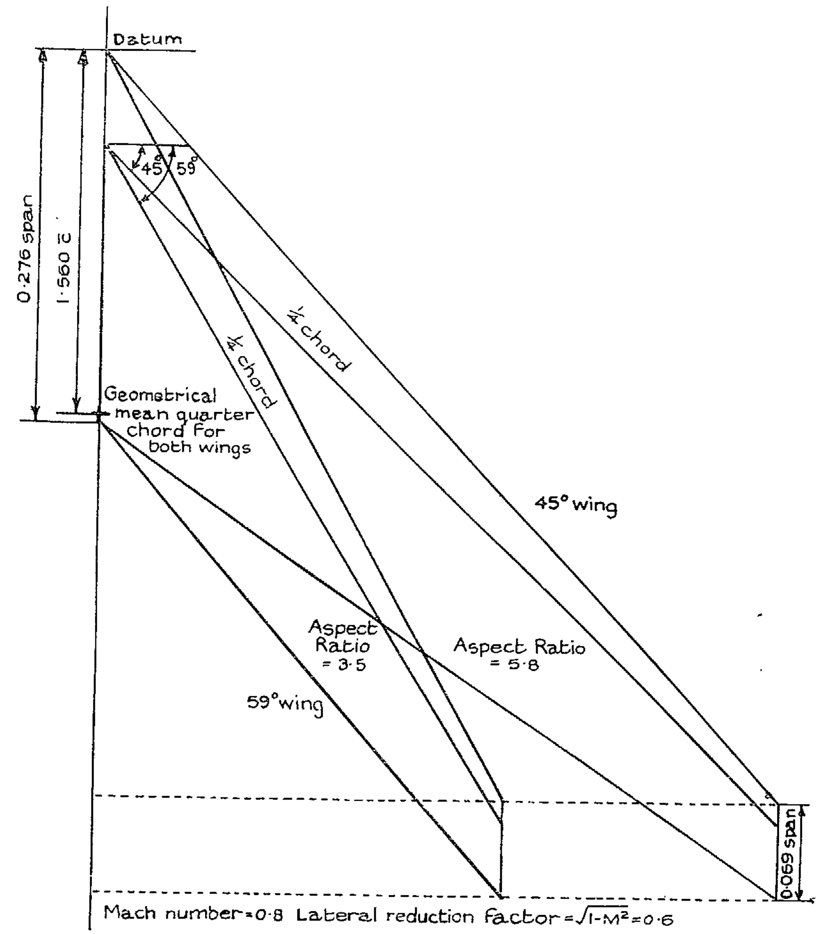

FIG. 2. Tapered wing with 45 deg sweepback before and after reduction of lateral dimensions in accordance with the Prandtl rule.

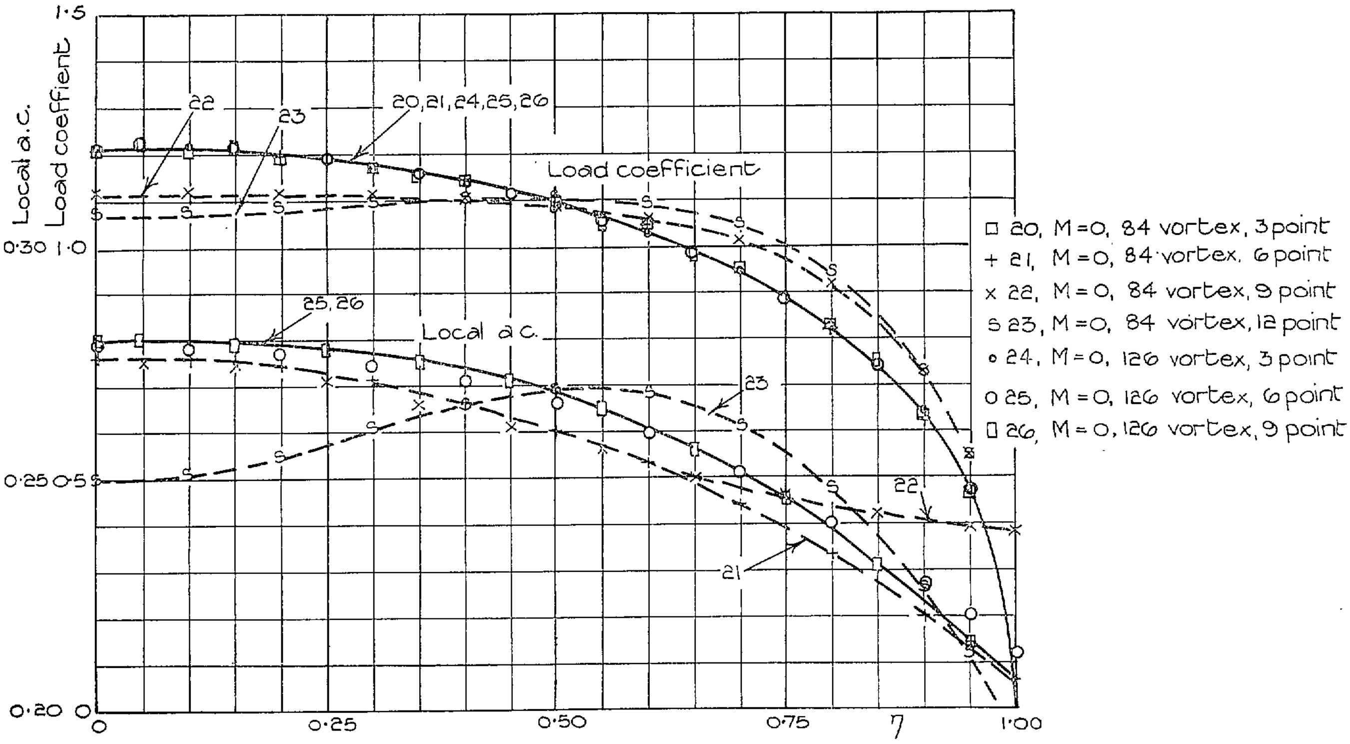

FIG. 3. Comparison of 84-vortex and 126-vortex standard solutions for 59 deg tapered wing : $M = 0$.

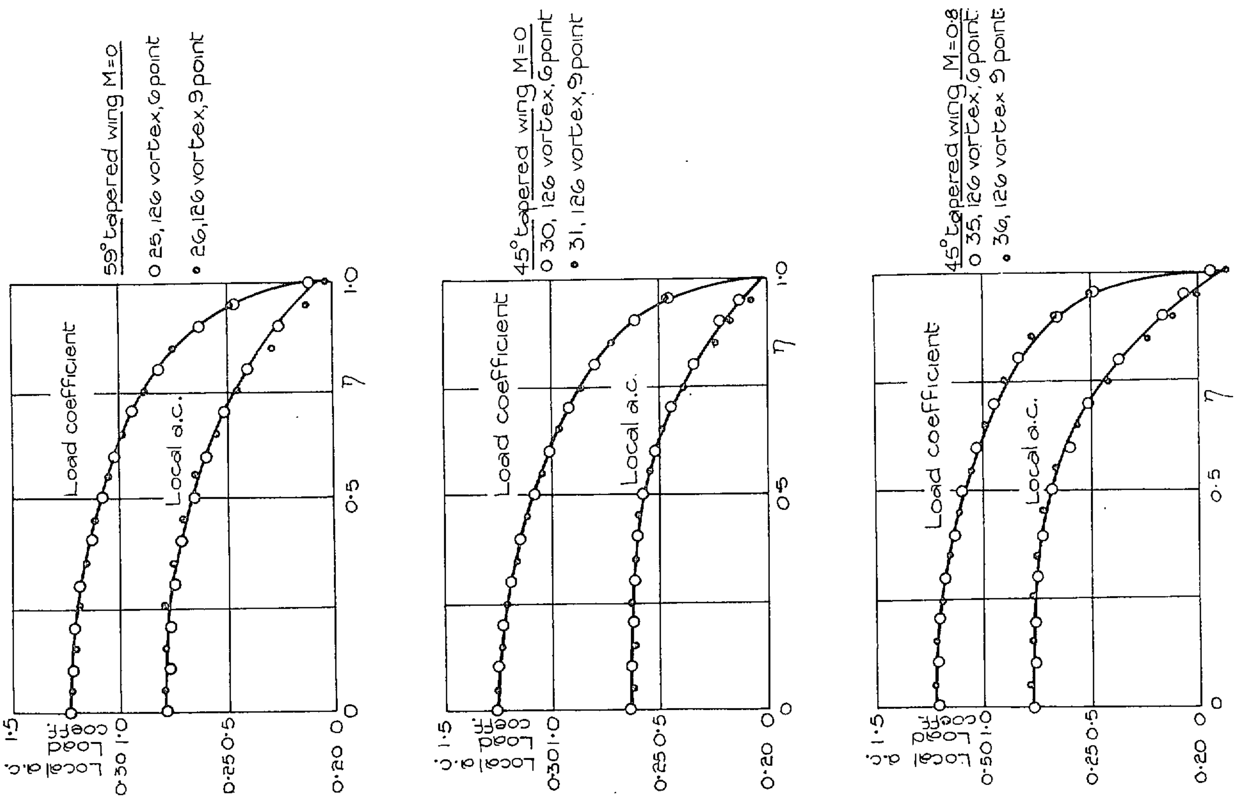

FIG. 4. Comparisons of six and nine-point standard solutions.

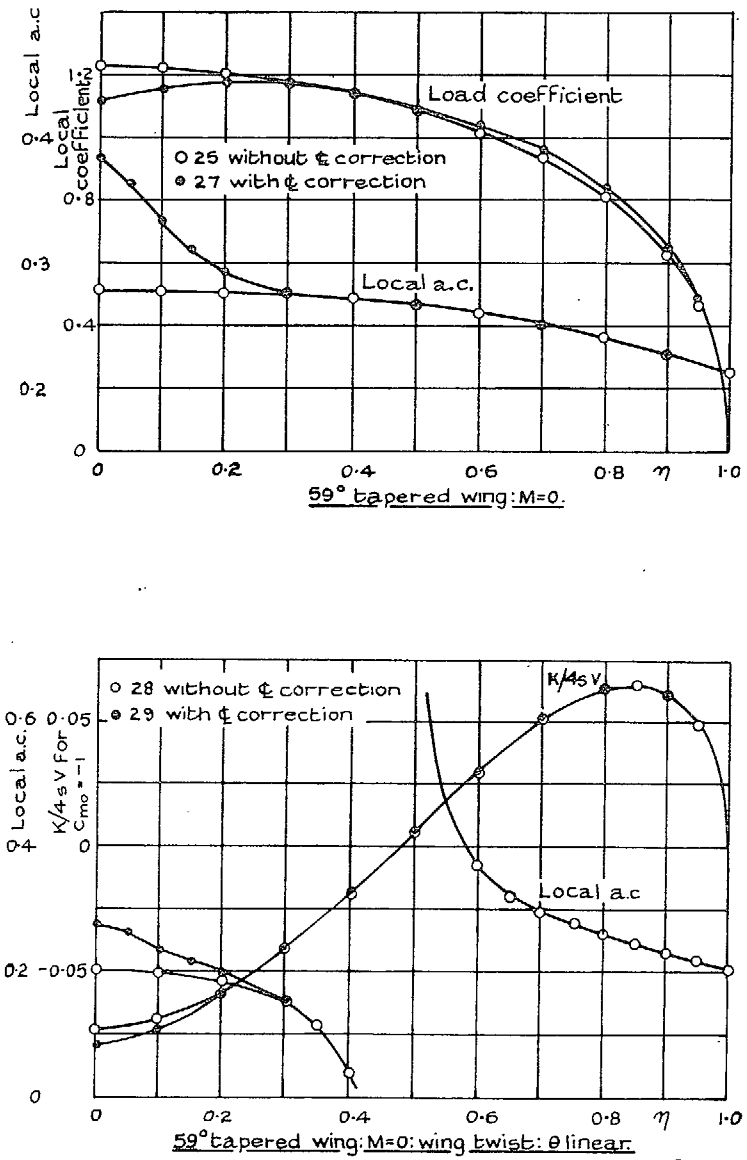

FIG. 5. Effect of centre-line correction on 126-vortex six-point solutions.

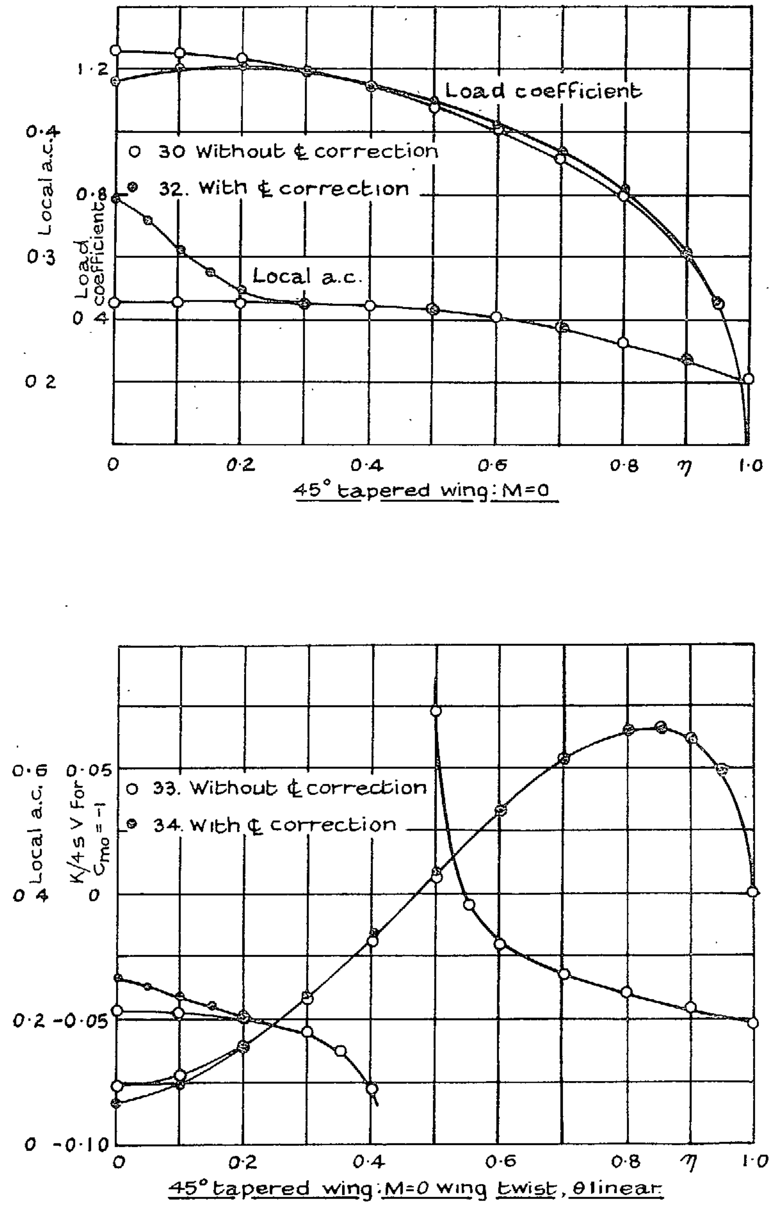

FIG. 6. Effects of centre-line correction on 126-vortex six-point solutions.

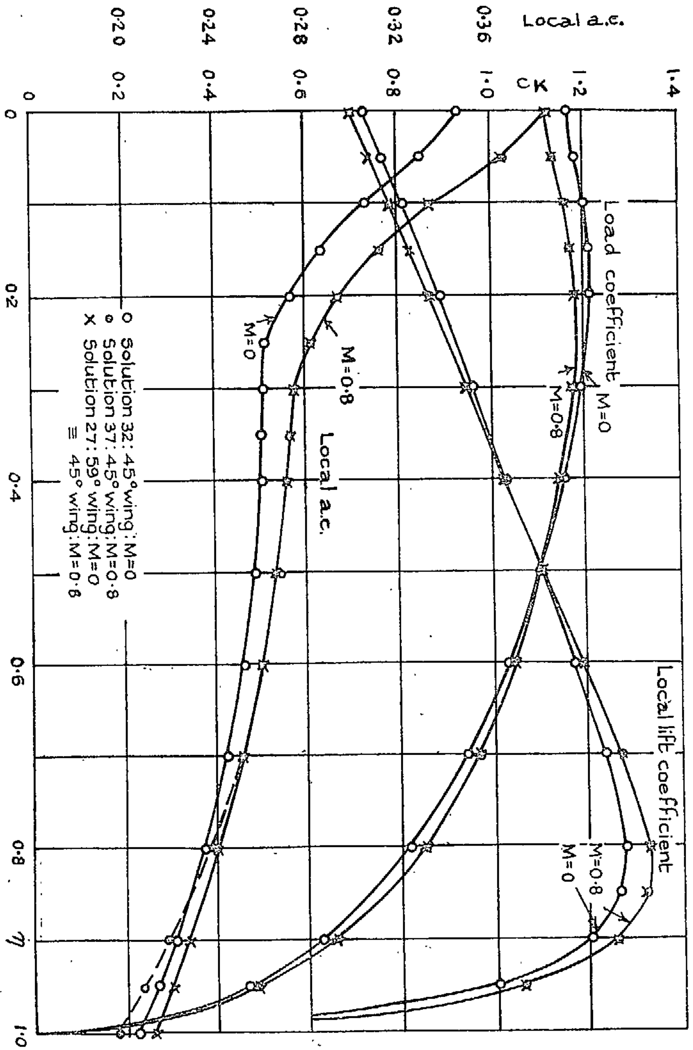

FIG. 8. Comparison of two methods of solution for compressible flow: 45 deg wing.

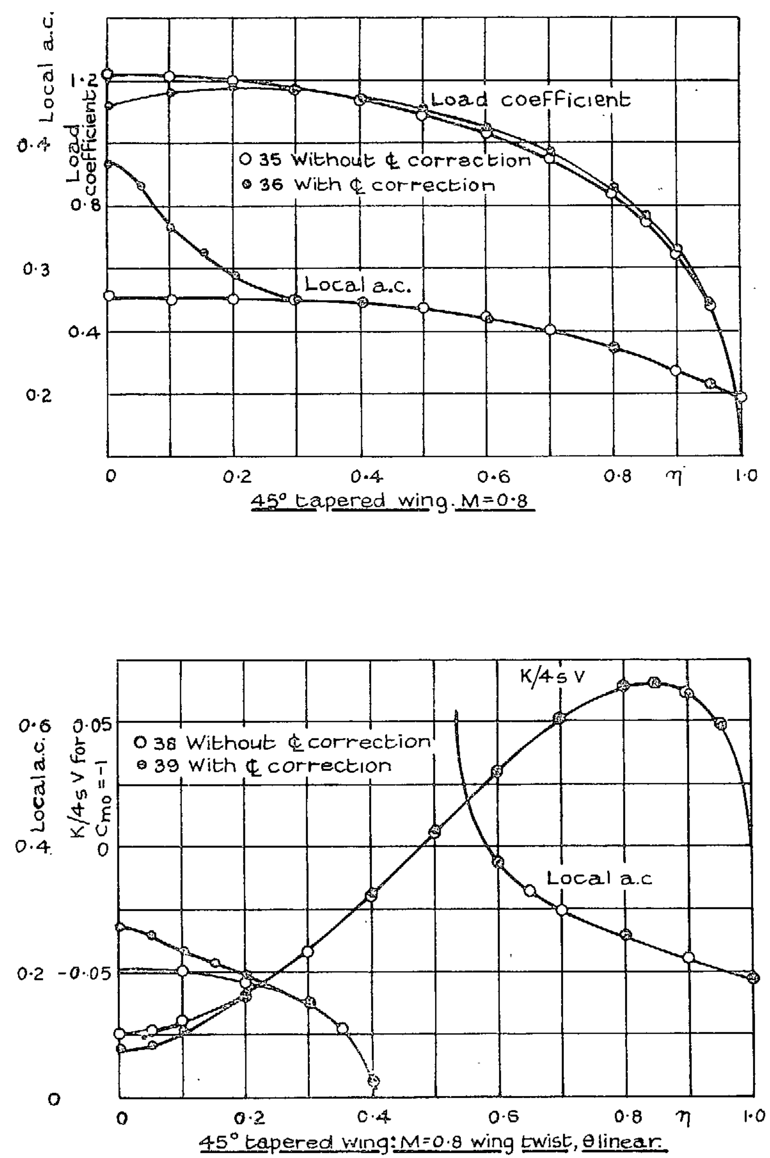

FIG. 7. Effect of centre-line corrections on 126-vortex six-point solutions.

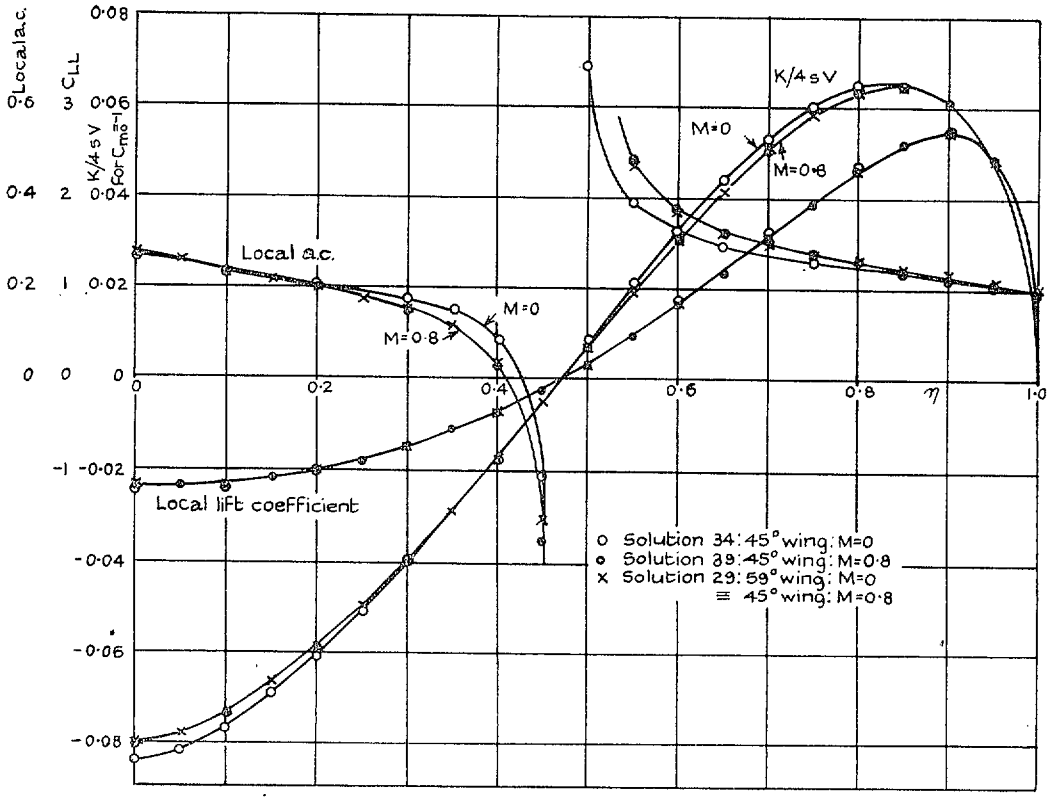

FIG. 9. Comparison of two methods of solution for compressible flow. Twisted wing at zero lift : θ linear.

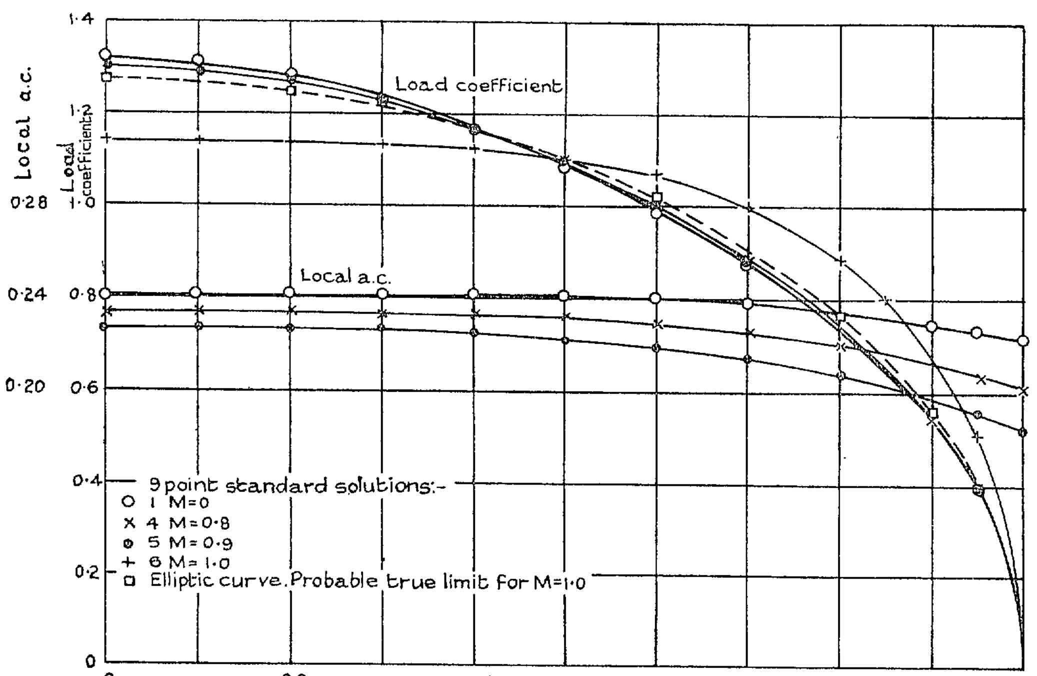

FIG. 10. Compressibility effects on straight tapered wing due to incidence.

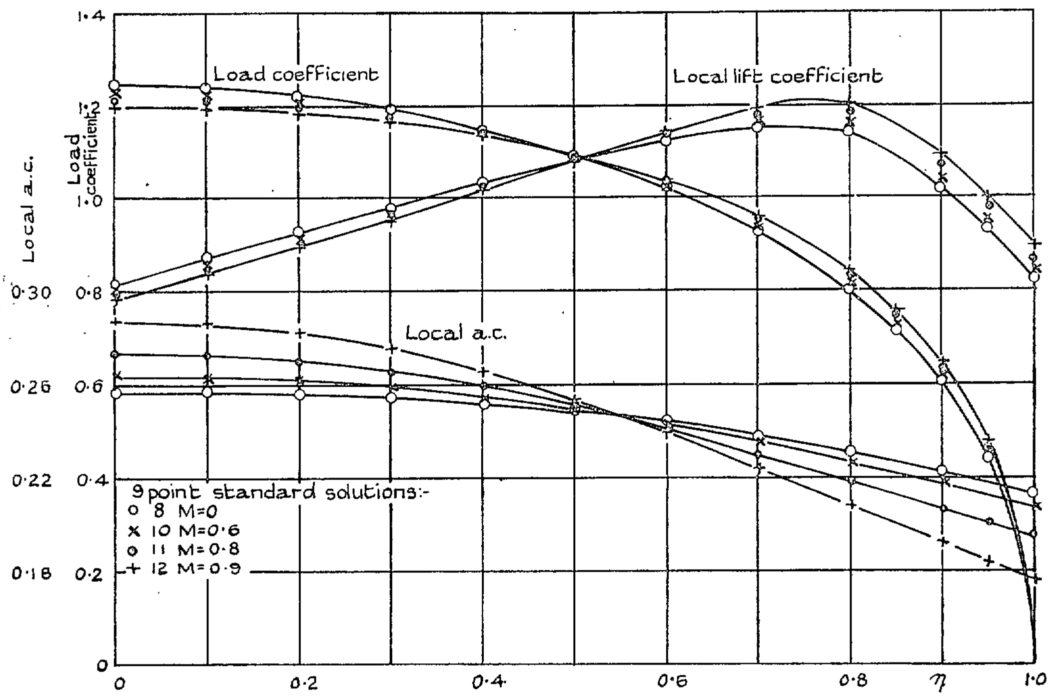

FIG. 11. Compressibility effects on tapered wing, 28·4 deg sweepback, due to incidence.

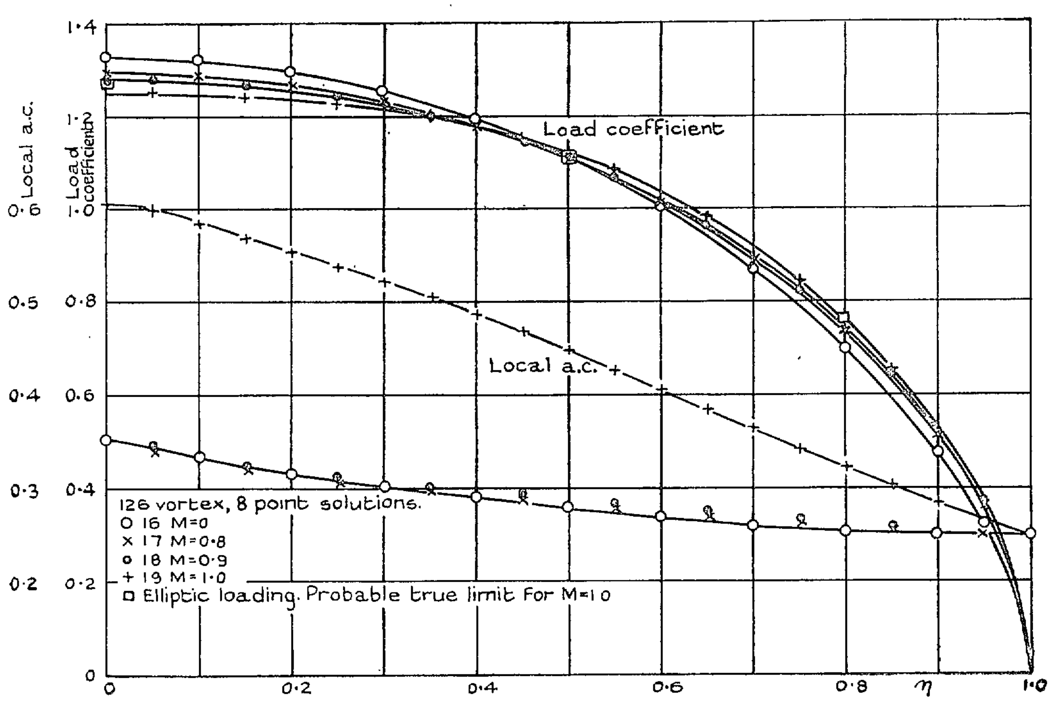

FIG. 12. Compressibility effects on triangular wing due to incidence.

APPENDIX

Note on Falkner's Method for Calculating Compressibility Effects on Wing Loading

By

W. P. Jones, M.A.,

of the Aerodynamics Division, N.P.L.

Summary.—The vortex-lattice method, as applied by Falkner[1] to estimate the effect of compressibility on wing loading, involves the use of an approximate formula for the downwash due to a 'rectangular vortex' in compressible flow. The exact expression for the downwash on the basis of linearised theory is given in this note, and a numerical comparison is made with the downwash values given by Falkner's formula. For Mach numbers up to $M = 0{\cdot}8$, and possibly higher values, the approximate formula appears to be quite satisfactory.

1. *Introduction.*—In Ref. 1, the vortex-lattice method of dealing with problems in incompressible flow[2] is adapted to the calculation of compressibility effects. As in the incompressible case, the downwash due to a continuous distribution of vorticity is represented as being due to a discontinouus system of rectangular vortices. The downwash field due to a unit rectangular vortex is first determined, and, by the use of the lattice method, solutions are then readily derived without the need for changing the dimensions of the wing for each Mach number[3]. In order to calculate the downwash distribution for a unit rectangular vortex* in compressible flow, Falkner makes the following basic assumptions:—

(i) that the downwash due to the transverse element of the vortex is $\sqrt{(1 - M^2)}$ times that given by incompressible flow theory,

(ii) that the downwash induced by the trailing elements is unaffected by compressibility.

On the basis of these assumptions he derives an approximate formula for the downwash which involves β $(\equiv\sqrt{(1 - M^2)})$ as a factor only. (*See* equation (10).)

It is well known that (i) is true for an infinitely long vortex, and that (ii) is true in the lifting-line case when the downwash points are on the line, which is itself assumed to be at right-angles to the direction of flow. In general, however, the assumptions made are not strictly valid, and this note investigates the extent to which they are approximately true in practice. The *exact* formula for the downwash due to a rectangular vortex is derived and a numerical comparison is made in Table 1 with the results given by the approximate formula used by Falkner.

2. *Theory.*—Let Ox, Oy, Oz be the axes of co-ordinates as indicated in Fig. 13, and let the wing lie in the plane $z = 0$ as shown

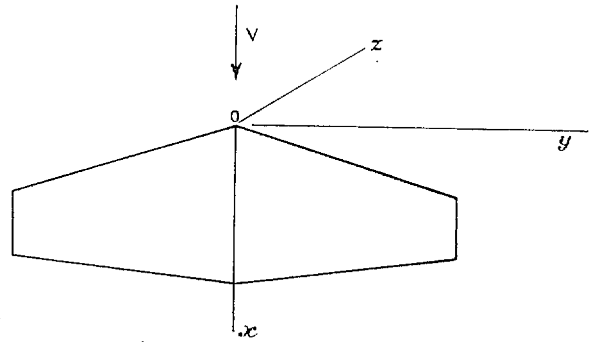

Fig. 13.

* *See* section 3c.

Then, if ϕ is the velocity potential of the disturbed flow produced by a small change of incidence, it will satisfy the equation

$$\beta^2 \frac{\partial^2\phi}{\partial x^2} + \frac{\partial^2\phi}{\partial y^2} + \frac{\partial^2\phi}{\partial z^2} = 0. \qquad (1)$$

The lift at any point is given simply by

$$p_b - p_a = \rho V \frac{\partial}{\partial x} (\phi_a - \phi_b), \qquad (2)$$

where p represents the pressure and the suffices a and b refer to the upper and lower sides of the plane $z = 0$ respectively. In the wake, there is no discontinuity in pressure, and, by equation (2), the discontinuity in ϕ must be a function of y only. Over the surface of the wing the downwash w ($\equiv \partial\phi/\partial z$) is known.

Let K represent the discontinuity $\phi_a - \phi_b$ in the velocity potential at points on the surface of the wing and the wake. The solution of equation (1) is then given by

$$4\pi\phi(x_0, y_0, z_0) = \iint K(x, y) \frac{\partial}{\partial z_0}\left(\frac{1}{r}\right) dx\, dy, \qquad (3)$$

where $r^2 \equiv (x_0 - x)^2 + \beta^2(y_0 - y)^2 + \beta^2 z_0^2$. Formula (3) gives ϕ as the velocity potential due to a distribution of compressibility doublets of strength K over the wing and the wake. When $M = 0$, $\beta = 1$, and formula (3) reduces to the usual form of the incompressible flow solution[4]. Since w is known over the wing, K can be determined from the integral equation

$$4\pi w(x_0, y_0, z_0) = -\iint K(x, y) \frac{\partial}{\partial z_0}\left(\frac{\beta^2 z_0}{r^3}\right) dx\, dy, \qquad (4)$$

where $z_0 \to 0$.

In general, K is a function of x and y over the wing, and, by equation (2), it is a function of y only in the wake. This note, however, is concerned with the following particular cases only: (a) the two-dimensional problem where K is a function of x only; (b) the lifting-line problem where K is a function of y; and (c) K = constant over a rectangular strip. Case (c) corresponds to that of the rectangular vortex in incompressible flow.

3. *Applications of Theory.* (a) *Two-dimensional Problem.*—In this case, equation (4) yields

$$4\pi w = -\int_0^\infty K(x) \frac{\partial}{\partial z_0}\left(\frac{\beta^2 z_0}{(x_0 - x)^2 + \beta^2 z_0^2}\right) \int_{-\infty}^\infty \frac{\partial}{\partial y}\left(\frac{y}{r}\right) dy\, dx.$$

$$= -2\int_0^\infty K(x) \frac{\partial}{\partial z_0}\left(\frac{\beta z_0}{(x_0 - x)^2 + \beta^2 z_0^2}\right) dx$$

$$= -2\int_0^\infty K(x) \frac{\partial}{\partial x}\left(\frac{\beta\,(x_0 - x)}{(x_0 - x)^2 + \beta^2 z_0^2}\right) dx. \qquad (5)$$

Since $K(o) = 0$ at the leading edge, integration by parts gives in the limit when $z_0 = 0$,

$$2\pi w = \beta \int_0^c \frac{\partial K}{\partial x}\left(\frac{1}{x_0 - x}\right) dx. \qquad (6)$$

The integral extends over the aerofoil chord only, as $\partial K/\partial x=0$ in the wake. Equation (6) implies that the downwash at a point on the aerofoil due to an infinite vortex of strength $\partial K/\partial x$ in compressible flow is the same as that due to one of strength $\beta(\partial K/\partial x)$ in incompressible flow. It is shown in section 3(c) that this conclusion does not apply when the transverse vortex is of finite length.

(b) *Lifting Line Problem.*—The doublet distribution K is in this case a function of y only, and extends, as shown in Fig. 14, from the lifting line $x = 0$ to $x = \infty$ between the lines $y = \pm s$.

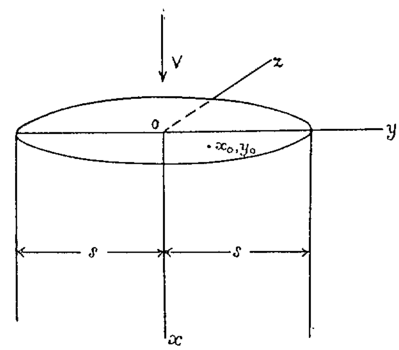

FIG. 14.

The downwash at a point x_0, y_0 not on the lifting line is given by equation (4) and can be expressed in the following form after integration with respect ot x, namely,

$$4\pi w(x_0, y_0) = -\int_{-s}^{s} K(y) \frac{\partial}{\partial z_0} \left\{ \frac{z_0}{(y_0 - y)^2 + z_0^2} \left[1 + \frac{x_0}{(x_0^2 + \beta^2(y_0 - y)^2 + \beta^2 z_0^2)^{1/2}} \right] \right\} dy.$$

Since $K(s) = K(-s) = 0$, this gives by integration by parts,

$$4\pi w = -\int_{-s}^{s} K(y) \left[1 + \frac{x_0}{[x_0^2 + \beta^2(y_0 - y)^2]^{1/2}} \right] \frac{\partial}{\partial y} \left(\frac{y_0 - y}{(y_0 - y)^2 + z_0^2} \right) dy$$

$$= \int_{-s}^{s} \frac{1}{(y_0 - y)} \frac{\partial}{\partial y} \left\{ K(y) \left[1 + \frac{x_0}{[x_0^2 + \beta^2(y_0 - y)^2]^{1/2}} \right] \right\} dy. \quad \ldots \quad \ldots \quad (7)$$

For points on the lifting line, $x_0 = 0$, and equation (7) yields

$$4\pi w(y_0) = \int_{-s}^{s} \frac{\partial K}{\partial y} \left(\frac{1}{y_0 - y} \right) dy. \quad \ldots \quad \ldots \quad \ldots \quad \ldots \quad (8)$$

Hence, as far as the value of the downwash along the lifting line is concerned, there is no compressibility effect. When $x_0 \neq 0$, however, the downwash is given by equation (7) and is influenced by the value of β.

(c) *Rectangular Doublet Strip.*—In incompressible flow, the downwash induced by a rectangular strip covered with a layer of doublets of constant strength K is the same as that induced by a rectangular vortex of strength K round the boundary. Let us next consider the downwash due to a doublet layer of this type in compressible flow.

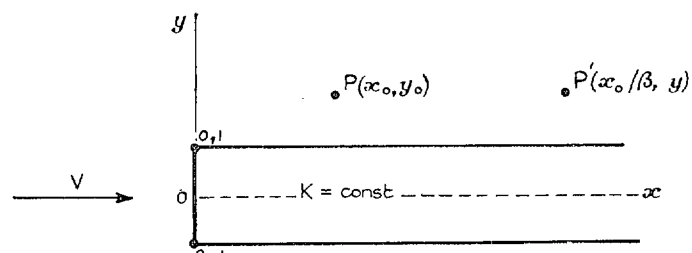

FIG. 15.

At any general point P the downwash induced by a doublet layer of unit strength* can, by the use of equation (7), be expressed in the form

$$4\pi w = \int_{-1}^{1} \int_{0}^{\infty} \frac{\partial}{\partial z_0} \left\{ \frac{z_0}{(y_0 - y)^2 + z_0^2} \frac{\partial}{\partial x} \left(\frac{x_0 - x}{r} \right) \right\} dx\, dy$$

* By analogy with incompressible-flow theory, the effect of the layer is assumed to correspond to that of the so-called rectangular vortex in compressible flow.

$$= -\int_{-1}^{1} \left[1 + \frac{x_0}{[x_0^2 + \beta^2(y_0 - y)^2]^{1/2}}\right] \frac{\partial}{\partial y}\left(\frac{y_0 - y}{(y_0 - y)^2 + z_0^2}\right) dy.$$

Integration with respect to y then yields

$$4\pi w(x_0,y_0) = \frac{1}{(y_0 + 1)}\left[1 + \frac{x_0}{[x_0^2 + \beta^2(y_0 + 1)^2]^{1/2}}\right]$$
$$- \frac{1}{(y_0 - 1)}\left[1 + \frac{x_0}{[x_0^2 + \beta^2(y_0 - 1)^2]^{1/2}}\right]$$
$$+ \frac{\beta^2}{x_0}\left[\frac{y_0 + 1}{[x_0^2 + \beta^2(y_0 + 1)^2]^{1/2}} - \frac{y_0 - 1}{[x_0^2 + \beta^2(y_0 - 1)^2]^{1/2}}\right]. \quad .. \quad (9)$$

When $\beta = 1$, equation (9) reduces to the well-known formula for the downwash due to a rectangular vortex in incompressible flow. The first two terms give the downwash contribution of the trailing vortices, and the third term corresponds to the transverse vortex. It should be noted that the downwash at P(x_0, y_0) in compressible flow due to a unit doublet strip is the same as that at P′(x_0/β, y) in incompressible flow[3]. (*See* Fig. 15.)

4. *Falkner's Formula.*—To obtain a solution of equation (4) for a particular wing, Falkner employs the vortex-lattice method. The doublet or circulation distribution K is first represented by a finite number of superimposed rectangular doublet layers (equivalent to rectangular vortices in the incompressible case). The downwash at a pivotal point is then given in terms of the contributions due to each rectangular layer. Instead of using equation (9), however, Falkner makes use of the results of section 3(a) and (b) and assumes that the downwash in compressible flow is given to sufficient accuracy by the formula

$$4\pi w_F = \frac{1}{(y_0 + 1)}\left[1 + \frac{x_0}{[x_0^2 + (y_0 + 1)^2]^{1/2}}\right]$$
$$- \frac{1}{(y_0 - 1)}\left[1 + \frac{x_0}{[x_0^2 + (y_0 - 1)^2]^{1/2}}\right]$$
$$+ \frac{\beta}{x_0}\left[\frac{y_0 + 1}{[x_0^2 + (y_0 + 1)^2]^{1/2}} - \frac{y_0 - 1}{[x_0^2 + (y_0 - 1)^2]^{1/2}}\right]. \quad .. \quad .. \quad .. \quad (10)$$

This corresponds to the incompressible-flow formula except that the effect of the transverse vortex is multiplied by β.

When x_0 is small compared to $\beta|(y_0 - 1)|$

$$4\pi w_F \to \frac{\beta}{x_0}\left(1 - \frac{y_0 - 1}{|y_0 - 1|}\right) + \frac{1}{(y_0 + 1)} - \frac{1}{(y_0 - 1)}$$
$$+ x_0\left(1 - \frac{\beta}{2}\right)\left[\frac{1}{(y_0 + 1)^2} - \frac{1}{(y_0 - 1)|(y_0 - 1)|}\right] \quad .. \quad .. \quad .. \quad (11)$$

and

$$4\pi w_E \to \frac{\beta}{x_0}\left(1 - \frac{y_0 - 1}{|(y_0 - 1)|}\right) + \frac{1}{y_0 + 1} - \frac{1}{y_0 - 1}$$
$$+ \frac{x_0}{2\beta}\left[\frac{1}{(y_0 + 1)^2} - \frac{1}{(y_0 - 1)|(y_0 - 1)|}\right]. \quad .. \quad .. \quad .. \quad .. \quad (12)$$

Hence the difference

$$4\pi(W_F - W_E) \to x_0 \left(\frac{2\beta - 1 - \beta^2}{2\beta}\right) \left[\frac{1}{(y_0 + 1)^2} - \frac{1}{(y_0 - 1)|(y_0 - 1)|}\right]. \quad \ldots \quad \ldots \quad (13)$$

In applications of the lattice theory, $y_0 \neq 1$ and usually has the values 0, 2, 4, 6 . . . etc.

A comparison between values of W_F and the exact downwash W_E given by equation (9) is made in Table 1 for different values of M at a number of points in the field of flow.

Concluding Remarks.—The formula for W_E and W_F show good agreement up to $M = 0 \cdot 8$, but for $M = 0 \cdot 9$ the differences are appreciable and they get larger as M tends to unity. The effect of these errors on the final solution for K and $p_b - p_a$ may tend to cancel, but until a check on the accuracy is made, results obtained by the use of equation (10) for values of $M > 0 \cdot 8$ should not be accepted without some element of doubt, particularly as the linearised thin-wing theory may then also be inadequate. For lower values of M, the use of equation (10) instead of (9) appears to be justified, and any results obtained would be subject mainly to possible errors inherent in the lattice method. Since the terms independent of β in formula (10) can be tabulated once and for all, it has great advantages from the computational point of view.

6. *Acknowledgement.*—The tabulated values given in this note were calculated by Miss Sylvia W. Skan.

REFERENCES

No.	*Author*	*Title, etc.*
1	V. M. Falkner	Calculations of Compressibility Effects on the Loading of a Swept-back Wing. December, 1945. A.R.C. 9261.
2	V. M. Falkner	The Calculation of Aerodynamic Loading on Surfaces of any Shape. R. & M. 1910. August, 1943.
3	R. Dickson	The Relationship between the Compressible Flow round a Swept-back Aerofoil and the Incompressible Flow round Equivalent Aerofoils. R.A.E. Report Aero. 2146. August, 1946. A.R.C. 9986. (Unpublished.)
4	W. P. Jones	Theoretical Determination of the Pressure Distribution on a Finite Wing in Steady Motion. R. & M. 2145. May, 1943.

TABLE 1

Values of $4\pi w_E$ and $4\pi w_F$

$M = 0 \cdot 6$

y_0 / x_0	0	2	4	6	10	20	40	Down-wash
10	4·0064	− 1·3271	− 0·2607	− 0·1087	− 0·0360	− 0·0076	− 0·0016	$4\pi w_E$
	4·0059	− 1·3274	− 0·2609	− 0·1088	− 0·0360	− 0·0076	− 0·0015	$4\pi w_F$
5	4·0254	− 1·3097	− 0·2469	− 0·0987	− 0·0310	− 0·0065	− 0·0014	$4\pi w_E$
	4·0238	− 1·3105	− 0·2469	− 0·0985	− 0·0307	− 0·0065	− 0·0014	$4\pi w_F$
2	4·1541	− 1·2231	− 0·2067	− 0·0796	− 0·0251	− 0·0056	− 0·0014	$4\pi w_E$
	4·1466	− 1·2223	− 0·2053	− 0·0789	− 0·0250	− 0·0056	− 0·0013	$4\pi w_F$
1	4·5614	− 1·0807	− 0·1754	− 0·0691	− 0·0227	− 0·0053	− 0·0012	$4\pi w_E$
	4·5456	− 1·0751	− 0·1739	− 0·0687	− 0·0226	− 0·0053	− 0·0012	$4\pi w_F$
0·5	5·7736	− 0·9192	− 0·1552	− 0·0632	− 0·0216	− 0·0051	− 0·0016	$4\pi w_E$
	5·7566	− 0·9119	− 0·1544	− 0·0630	− 0·0216	− 0·0049	− 0·0012	$4\pi w_F$
0	2	− 0·6667	− 0·1333	− 0·0571	− 0·0202	− 0·0050	− 0·0012	$4\pi w_E$
	2	− 0·6667	− 0·1333	− 0·0571	− 0·0202	− 0·0050	− 0·0012	$4\pi w_F$
− 0·5	− 1·7736	− 0·4142	− 0·1114	− 0·0510	− 0·0188	− 0·0049	− 0·0008	$4\pi w_E$
	− 1·7566	− 0·4215	− 0·1122	− 0·0512	− 0·0188	− 0·0051	− 0·0012	$4\pi w_F$
− 1	− 0·5614	− 0·2527	− 0·0912	− 0·0451	− 0·0177	− 0·0047	− 0·0012	$4\pi w_E$
	− 0·5456	− 0·2583	− 0·0927	− 0·0455	− 0·0178	− 0·0047	− 0·0012	$4\pi w_F$
− 2	− 0·1541	− 0·1103	− 0·0599	− 0·0346	− 0·0153	− 0·0044	− 0·0010	$4\pi w_E$
	− 0·1466	− 0·1111	− 0·0613	− 0·0353	− 0·0154	− 0·0044	− 0·0011	$4\pi w_F$
− 5	− 0·0254	− 0·0237	− 0·0197	− 0·0155	− 0·0094	− 0·0035	− 0·0010	$4\pi w_E$
	− 0·0238	− 0·0229	− 0·0197	− 0·0157	− 0·0097	− 0·0035	− 0·0010	$4\pi w_F$
− 10	− 0·0064	− 0·0063	− 00·059	− 0·0055	− 0·0044	− 0·0024	− 0·0008	$4\pi w_E$
	− 0·0059	− 0·0060	− 0·0057	− 0·0054	− 0·0044	− 0·0024	− 0·0009	$4\pi w_F$

TABLE 1—*continued*

Values of $4\pi w_E$ *and* $4\pi w_F$

$M = 0\cdot8$

y_0 / x_0	0	2	4	6	10	20	40	Down-wash
10	4·0036	− 1·3298	− 0·2632	− 0·1109	− 0·0375	− 0·0082	− 0·0017	$4\pi w_E$
	4·0019	− 1·3312	− 0·2641	− 0·1113	− 0·0374	− 0·0080	− 0·0016	$4\pi w_F$
5	4·0146	− 1·3197	− 0·2543	− 0·1039	− 0·0332	− 0·0069	− 0·0014	$4\pi w_E$
	4·0081	− 1·3232	− 0·2546	− 0·1028	− 0·0322	− 0·0067	− 0·0014	$4\pi w_F$
2	4·0880	− 1·2623	− 0·2212	− 0·0854	− 0·0266	− 0·0058	− 0·0013	$4\pi w_E$
	4·0571	− 1·2608	− 0·2150	− 0·0822	− 0·0258	− 0·0057	− 0·1003	$4\pi w_F$
1	4·3324	− 1·1465	− 0·1872	− 0·0728	− 0·0235	− 0·0054	− 0·0013	$4\pi w_E$
	4·2627	− 1·1235	− 0·1803	− 0·0705	− 0·0230	− 0·0053	− 0·0013	$4\pi w_F$
0·5	5·1242	− 0·9834	− 0·1621	− 0·0652	− 0·0219	− 0·0052	− 0·0014	$4\pi w_E$
	5·0411	− 0·9487	− 0·1579	− 0·0639	− 0·0218	− 0·0050	− 0·0012	$4\pi w_F$
0	2	− 0·6667	− 0·1333	− 0·0571	− 0·0202	− 0·0050	− 0·0012	$4\pi w_E$
	2	− 0·6667	− 0·1333	− 0·0571	− 0·0202	− 0·0050	− 0·0012	$4\pi w_F$
− 0·5	− 1·1242	− 0·3500	− 0·1045	− 0·0490	− 0·0185	− 0·0048	− 0·0010	$4\pi w_E$
	− 1·0411	− 0·3847	− 0·1087	− 0·0503	− 0·0186	− 0·0050	− 0·0012	$4\pi w_F$
− 1	− 0·3324	− 0·1869	− 0·0794	− 0·0414	− 0·0169	− 0·0046	− 0·0011	$4\pi w_E$
	− 0·2627	− 0·2099	− 0·0863	− 0·0437	− 0·0174	− 0·0047	− 0·0011	$4\pi w_F$
− 2	− 0·0880	− 0·0711	− 0·0454	− 0·0288	− 0·0138	− 0·0042	− 0·0011	$4\pi w_E$
	− 0·0571	− 0·0726	− 0·0516	− 0·0320	− 0·0146	− 0·0043	− 0·0011	$4\pi w_F$
− 5	− 0·0146	− 0·0137	− 0·0123	− 0·0103	− 0·0072	− 0·0031	− 0·0010	$4\pi w_E$
	− 0·0081	− 0·0102	− 0·0120	− 0·0114	− 0·0082	− 0·0033	− 0·0010	$4\pi w_F$
− 10	− 0·0036	− 0·0036	− 0·0034	− 0·0033	− 0·0029	− 0·0018	− 0·0007	$4\pi w_E$
	− 0·0019	− 0·0022	− 0·0025	− 0·0029	− 0·0030	− 0·0020	− 0·0008	$4\pi w_F$

TABLE 1—*continued*

Values of $4\pi w_E$ *and* $4\pi w_F$

$M = 0{\cdot}9$

y_0 / x_0	0	2	4	6	10	20	40	Down-wash
10	4·0018	− 1·3314	− 0·2647	− 0·1124	− 0·0387	− 0·0088	− 0·0018	$4\pi w_E$
	3·9987	− 1·3343	− 0·2667	− 0·1134	− 0·0385	− 0·0082	− 0·0016	$4\pi w_F$
5	4·0075	− 1·3260	− 0·2596	− 0·1079	− 0·0355	− 0·0075	− 0·0015	$4\pi w_E$
	3·9952	− 1·3336	− 0·2609	− 0·1062	− 0·0334	− 0·0069	− 0·0014	$4\pi w_F$
2	4·0470	− 1·2920	− 0·2357	− 0·0923	− 0·0287	− 0·0061	− 0·0013	$4\pi w_E$
	3·9837	− 1·2924	− 0·2229	− 0·0849	− 0·0264	− 0·0058	− 0·0013	$4\pi w_F$
1	4·1817	− 1·2088	− 0·2024	− 0·0780	− 0·0247	− 0·0055	− 0·0012	$4\pi w_E$
	4·0306	− 1·1631	− 0·1856	− 0·0721	− 0·0233	− 0·0054	− 0·0013	$4\pi w_F$
0·5	4·6534	− 1·0600	− 0·1723	− 0·0681	− 0·0225	− 0·0053	− 0·0013	$4\pi w_E$
	4·4539	− 0·9789	− 0·1607	− 0·0647	− 0·0219	− 0·0051	− 0·0012	$4\pi w_F$
0	2	− 0·6667	− 0·1333	− 0·0571	− 0·0202	− 0·0050	− 0·0012	$4\pi w_E$
	2	− 0·6667	− 0·1333	− 0·0571	− 0·0202	− 0·0050	− 0·0012	$4\pi w_F$
− 0·5	− 0·6534	− 0·2734	− 0·0943	− 0·0461	− 0·0179	− 0·0047	− 0·0011	$4\pi w_E$
	− 0·4539	− 0·3545	− 0·1059	− 0·0495	− 0·0185	− 0·0049	− 0·0012	$4\pi w_F$
− 1	− 0·1817	− 0·1246	− 0·0642	− 0·0362	− 0·0157	− 0·0045	− 0·0012	$4\pi w_E$
	− 0·0306	− 0·1703	− 0·0810	− 0·0421	− 0·0171	− 0·0046	− 0·0011	$4\pi w_F$
− 2	− 0·0470	− 0·0414	− 0·0309	− 0·0219	− 0·0117	− 0·0039	− 0·0011	$4\pi w_E$
	+ 0·0163	− 0·0410	− 0·0437	− 0·0293	− 0·0140	− 0·0042	− 0·0011	$4\pi w_F$
− 5	− 0·0075	− 0·0074	− 0·0070	− 0·0063	− 0·0049	− 0·0025	− 0·0009	$4\pi w_E$
	+ 0·0048	+ 0·0002	− 0·0057	− 0·0080	− 0·0070	− 0·0031	− 0·0010	$4\pi w_F$
− 10	− 0·0018	− 0·0020	− 0·0019	− 0·0018	− 0·0017	− 0·0012	− 0·0006	$4\pi w_E$
	+ 0·0013	+ 0·0009	+ 0·0001	− 0·0008	− 0·0019	− 0·0018	− 0·0008	$4\pi w_F$

TABLE 1—*continued*

Values of $4\pi w_E$ *and* $4\pi w_F$

$M = 0{\cdot}95$

y_0 / x_0	0	2	4	6	10	20	40	Down-wash
10	4·0009	− 1·3324	− 0·2656	− 0·1133	− 0·0395	− 0·0092	− 0·0019	$4\pi w_E$
	3·9962	− 1·3366	− 0·2687	− 0·1150	− 0·0394	− 0·0085	− 0·0017	$4\pi w_F$
5	4·0038	− 1·3295	− 0·2629	− 0·1107	− 0·0374	− 0·0081	− 0·0016	$4\pi w_E$
	3·9855	− 1·3415	− 0·2657	− 0·1088	− 0·0343	− 0·0070	− 0·0015	$4\pi w_F$
2	4·0242	− 1·3107	− 0·2476	− 0·0992	− 0·0312	− 0·0063	− 0·0014	$4\pi w_E$
	3·9284	− 1·3161	− 0·2289	− 0·0870	− 0·0268	− 0·0059	− 0·0013	$4\pi w_F$
1	4·0953	− 1·2577	− 0·2192	− 0·0845	− 0·0264	− 0·0058	− 0·0013	$4\pi w_E$
	3·8558	− 1·1930	− 0·1895	− 0·0732	− 0·0236	− 0·0054	− 0·0013	$4\pi w_F$
0·5	4·3580	− 1·1378	− 0·1855	− 0·0722	− 0·0235	− 0·0054	− 0·0013	$4\pi w_E$
	4·0116	− 1·0017	− 0·1628	− 0·0653	− 0·0220	− 0·0051	− 0·0012	$4\pi w_F$
0	2	− 0·6667	− 0·1333	− 0·0571	− 0·0202	− 0·0050	− 0·0012	$4\pi w_E$
	2	− 0·6667	− 0·1333	− 0·0571	− 0·0202	− 0·0050	− 0·0012	$4\pi w_F$
− 0·5	− 0·3580	− 0·1956	− 0·0811	− 0·0420	− 0·0169	− 0·0046	− 0·0011	$4\pi w_E$
	− 0·0116	− 0·3317	− 0·1038	− 0·0489	− 0·0184	− 0·0049	− 0·0012	$4\pi w_F$
− 1	− 0·0953	− 0·0757	− 0·0474	− 0·0297	− 0·0140	− 0·0042	− 0·0011	$4\pi w_E$
	+ 0·1442	− 0·1404	− 0·0771	− 0·0410	− 0·0168	− 0·0046	− 0·0011	$4\pi w_F$
− 2	− 0·0242	− 0·0227	− 0·0190	− 0·0150	− 0·0092	− 0·0037	− 0·0010	$4\pi w_E$
	+ 0·0716	− 0·0173	− 0·0377	− 0·0272	− 0·0136	− 0·0041	− 0·0011	$4\pi w_F$
− 5	− 0·0038	− 0·0039	− 0·0037	− 0·0035	− 0·0030	− 0·0019	− 0·0008	$4\pi w_E$
	+ 0·0145	+ 0·0081	− 0·0009	− 0·0054	− 0·0061	− 0·0030	− 0·0009	$4\pi w_F$
− 10	− 0·0009	− 0·0010	− 0·0010	− 0·0009	− 0·0009	− 0·0008	− 0·0005	$4\pi w_E$
	+ 0·0038	+ 0·0032	+ 0·0021	+ 0·0008	− 0·0010	− 0·0015	− 0·0007	$4\pi w_F$

TABLE 1—*continued*

Values of $4\pi w_E$ *and* $4\pi w_F$

$M = 1$

$4\pi w_E$

y_0 / x_0	0	2	4	6	10	20	40
> 0	4	− 1·3334	− 0·2666	− 0·1142	− 0·0404	− 0·0100	− 0·0024
= 0	2	− 0·6667	− 0·1333	− 0·0571	− 0·0202	− 0·0050	− 0·0012
< 0	0	0	0	0	0	0	0

$4\pi w_F$

y_0 / x_0	0	2	4	6	10	20	40
10	3·9900	− 1·3425	− 0·2737	− 0·1189	− 0·0416	− 0·0090	− 0·0018
5	3·9610	− 1·3614	− 0·2777	− 0·1155	− 0·0365	− 0·0074	− 0·0015
2	3·7888	− 1·3762	− 0·2439	− 0·0921	− 0·0280	− 0·0060	− 0·0013
1	3·4142	− 1·2684	− 0·1995	− 0·0761	− 0·0242	− 0·0055	− 0·0013
0·5	2·8944	− 1·0591	− 0·1682	− 0·0668	− 0·0222	− 0·0053	− 0·0012
0	2	− 0·6667	− 0·1333	− 0·0571	− 0·0202	− 0·0050	− 0·0012
− 0·5	1·1056	− 0·2743	− 0·0984	− 0·0474	− 0·0182	− 0·0047	− 0·0012
− 1	0·5858	− 0·0650	− 0·0671	− 0·0381	− 0·0162	− 0·0045	− 0·0011
− 2	0·2112	+ 0·0428	− 0·0227	− 0·0221	− 0·0124	− 0·0040	− 0·0011
− 5	0·0390	0·0280	+ 0·0111	+ 0·0013	− 0·0039	− 0·0026	− 0·0009
− 10	0·0100	0·0091	0·0071	0·0047	+ 0·0012	− 0·0010	− 0·0006

(22975) Wt. 15-680 K9 7/53 F. M. & S. PRINTED IN GREAT BRITAIN

D

R. & M. No. 2685
(11,944, 12,650, 12,147)
A.R.C. Technical Report

Publications of the Aeronautical Research Council

ANNUAL TECHNICAL REPORTS OF THE AERONAUTICAL RESEARCH COUNCIL (BOUND VOLUMES)

1936 Vol. I. Aerodynamics General, Performance, Airscrews, Flutter and Spinning. 40*s.* (40*s.* 9*d.*)
Vol. II. Stability and Control, Structures, Seaplanes, Engines, etc. 50*s.* (50*s.* 10*d.*)

1937 Vol. I. Aerodynamics General, Performance, Airscrews, Flutter and Spinning. 40*s.* (40*s.* 10*d.*)
Vol. II. Stability and Control, Structures, Seaplanes, Engines, etc. 60*s.* (61*s.*)

1938 Vol. I. Aerodynamics General, Performance, Airscrews. 50*s.* (51*s.*)
Vol. II. Stability and Control, Flutter, Structures, Seaplanes, Wind Tunnels, Materials. 30*s.* (30*s.* 9*d.*)

1939 Vol. I. Aerodynamics General, Performance, Airscrews, Engines. 50*s.* (50*s.* 11*d.*)
Vol. II. Stability and Control, Flutter and Vibration, Instruments, Structures, Seaplanes, etc. 63*s.* (64*s.* 2*d.*)

1940 Aero and Hydrodynamics, Aerofoils, Airscrews, Engines, Flutter, Icing, Stability and Control, Structures, and a miscellaneous section. 50*s.* (51*s.*)

1941 Aero and Hydrodynamics, Aerofoils, Airscrews, Engines, Flutter, Stability and Control, Structures. 63*s.* (64*s.* 2*d.*)

1942 Vol. I. Aero and Hydrodynamics, Aerofoils, Airscrews, Engines. 75*s.* (76*s.* 3*d.*)
Vol. II. Noise, Parachutes, Stability and Control, Structures, Vibration, Wind Tunnels. 47*s.* 6*d.* (48*s.* 5*d.*)

1943 Vol. I. (In the press.)
Vol. II. (In the press.)

ANNUAL REPORTS OF THE AERONAUTICAL RESEARCH COUNCIL—

1933-34	1*s.* 6*d.* (1*s.* 8*d.*)	1937	2*s.* (2*s.* 2*d.*)
1934-35	1*s.* 6*d.* (1*s.* 8*d.*)	1938	1*s.* 6*d.* (1*s.* 8*d.*)
April 1, 1935 to Dec. 31, 1936.	4*s.* (4*s.* 4*d.*)	1939-48	3*s.* (3*s.* 2*d.*)

INDEX TO ALL REPORTS AND MEMORANDA PUBLISHED IN THE ANNUAL TECHNICAL REPORTS AND SEPARATELY—

April, 1950 - - - - - R. & M. No. 2600. 2*s.* 6*d.* (2*s.* 7½*d.*)

AUTHOR INDEX TO ALL REPORTS AND MEMORANDA OF THE AERONAUTICAL RESEARCH COUNCIL—

1909-1949 - - - - - R. & M. No. 2570. 15*s.* (15*s.* 3*d.*)

INDEXES TO THE TECHNICAL REPORTS OF THE AERONAUTICAL RESEARCH COUNCIL—

December 1, 1936—June 30, 1939.	R. & M. No. 1850.	1*s.* 3*d.* (1*s.* 4½*d.*)
July 1, 1939—June 30, 1945.	R. & M. No. 1950.	1*s.* (1*s.* 1½*d.*)
July 1, 1945—June 30, 1946.	R. & M. No. 2050.	1*s.* (1*s.* 1½*d.*)
July 1, 1946—December 31, 1946.	R. & M. No. 2150.	1*s.* 3*d.* (1*s.* 4½*d.*)
January 1, 1947—June 30, 1947.	R. & M. No. 2250.	1*s.* 3*d.* (1*s.* 4½*d.*)
July, 1951.	R. & M. No. 2350.	1*s.* 9*d.* (1*s.* 10½*d.*)

Prices in brackets include postage.

Obtainable from

HER MAJESTY'S STATIONERY OFFICE

York House, Kingsway, London, W.C.2; 423 Oxford Street, London, W.1 (Post Orders: P.O. Box 569, London, S.E.1); 13a Castle Street, Edinburgh 2; 39 King Street, Manchester 2; 2 Edmund Street, Birmingham 3; 1 St. Andrew's Crescent, Cardiff; Tower Lane, Bristol 1; 80 Chichester Street, Belfast or through any bookseller.

S.O. Code No. 23-2685